
Towards deep observation: A systematic survey on artificial intelligence techniques to monitor fetus via Ultrasound Images

MAHMOOD ALZUBAIDI¹, MARCO AGUS¹, KHALID ALYAFEI^{2,3}, KHALED A ALTHELAYA¹, UZAIR SHAH¹, ALAA A. ABD-ALRAZAQ¹, MOHAMMED ANBAR³, MICHEL MAKHLOUF², AND MOWAFA HOUSEH¹

¹ College of Science and Engineering, Hamad Bin Khalifa University, Doha, Qatar; ² Weil Cornell Medical College-Qatar; ³Sidra Medical and Research Center, Doha, Qatar; ³National Advanced IPv6 Centre, University Sains Malaysia, Penang, Malaysia

Key words: fetal; fetus; ultrasound; artificial intelligence; deep learning; machine learning

Abstract

Objective: Developing innovative informatics approaches aimed to enhance fetal monitoring is a burgeoning field of study in reproductive medicine. Over the last decade, several reviews have been conducted regarding Artificial intelligence (AI) techniques to improve pregnancy outcomes. They are limited by focusing on specific data (e.g., electronic health records) or a mother's care during pregnancy. This survey aims to explore how artificial intelligence (AI) can assist with fetal growth monitoring via Ultrasound (US) image.

Materials and methods: We performed a systematic survey guided by the Joanna Briggs Institute Reviewer Manual. We reported our findings using the guidelines for PRISMA (Preferred Reporting Items for Systematic Reviews and Meta-Analysis). We conducted a comprehensive search of eight medical and computer science bibliographic databases, including PubMed, Embase, PsycINFO, ScienceDirect, IEEE explore, ACM Library, Google Scholar, and the Web of Science. We retrieved studies published between 2010 to 2021. The search terms were chosen based on the target intervention (i.e., AI and ultrasound images) and target population (i.e., fetal/fetus). Publications written in English that converged on AI techniques used to monitor fetal care during pregnancy regardless of target fetal disease or anatomy were included. Data extracted from studies were synthesized using a

narrative approach.

Results: Out of 1269 retrieved studies, we included 107 distinct studies from queries that were relevant to the topic in the survey. We found that 2D ultrasound images were more popular (n = 88) than 3D and 4D ultrasound images (n = 19). Classification is the most commonly used method (n = 42), followed by segmentation (n = 31), classification integrated with segmentation (n = 16) and other miscellaneous such as object-detection, regression and reinforcement learning (n = 18). The most common areas that gained traction within the pregnancy domain were the fetus head (n = 43), then fetus body (n=31), fetus heart (n=13), fetus abdomen (n=10), and lastly the fetus face (n=10). In the most recent studies, deep learning techniques were primarily used (n = 81), followed by machine learning (n=16), artificial neural network (n=7), and reinforcement learning (n=2). We did not find studies that developed AI-based applications at any medical center.

Conclusions: Overall, we found that AI techniques played a crucial role in predicting particular fetal diseases and identifying fetus anatomy structures during pregnancy. More research is required to validate this technology from a physician's perspective, such as pilot studies and randomized controlled trials on AI and its applications in a hospital setting. Additional research is required to focus in how radiologists can utilize AI technique because when AI is integrated into the clinical process as a tool to assist clinicians, more accurate and reproducible radiological assessments can be made.

1. Introduction

1.1 Background

Artificial Intelligence (AI) is a broad discipline that aims to replicate the inherent intelligence shown by people via artificial methods [1]. Recently, AI techniques have been widely utilized in

the medical sector [2]. Historically, AI techniques were stand-alone systems with no direct link to medical imaging. With the development of new technology, the idea of 'joint decision-making' between people and AI offers the potential of boosting high performance in the area of medical imaging [3].

Correspondence to: Dr. Mowafa Househ, College of Science and Engineering, Hamad Bin Khalifa University, Doha, Qatar

Tel.: +xxxxxxxxxxxxxxxxxxxxxx; E-mail: mhouseh@hbku.edu.qa

In computer science, Machine Learning (ML), Deep Learning (DL), Artificial Neural Network (ANN) and Reinforcement Learning (RL) are subset techniques of AI that are used to perform different tasks on medical images such as classification, segmentation, object identification, and regression [4]–[6]. Diagnosis using computer-aided detection (CAD) has moved towards becoming AI automated process in the medical images[7], which include most of the medical imaging data such as (X-ray radiography, Fluoroscopy, MRI, Medical ultrasonography or ultrasound, Endoscopy, Elastography, Tactile imaging, and Thermography) [8]. However, digitized medical images come with a plethora of new information, possibilities, and challenges. Therefore, AI techniques are able to address some of these challenges by showing impressive accuracy and sensitivity in identifying imaging abnormalities. These techniques promise to enhance tissue-based detection and characterization, with the potential to improve diagnoses of diseases [9].

At present, the use of AI techniques in medical images has been discussed in depth across many medical disciplines, including identifying cardiovascular abnormalities, detecting fractures and other musculoskeletal injuries, aiding in diagnosing neurological diseases, reducing thoracic complications and conditions, screening for common cancers, and many other prognoses and diagnosis tasks [7], [10]–[13]. Furthermore, AI techniques have shown the ability to provide promising findings when utilizing prenatal medical images, such as monitoring fetal development at each stage of pregnancy, predicting a pregnant placenta's health, and identifying potential complications [14]–[17]. AI techniques may assist with detecting several fetal diseases and adverse pregnancy outcomes with complex etiology and pathogenesis such as amniotic band syndrome, congenital diaphragmatic hernia, congenital high airway obstruction syndrome, fetal bowel obstruction, gastroschisis, omphalocele, pulmonary sequestration, and sacrococcygeal teratoma [18]–[20]. Therefore, more research is needed to understand the role of utilizing AI techniques in the early stage of pregnancy both to prevent and reduce unfavorable outcomes as well as provide an understanding of fetal anomalies and illnesses throughout pregnancy and for drastically reducing the need of more invasive diagnostic procedures that may be harmful for the fetus [21].

Various imaging modalities (e.g., Ultrasound, MRI, and computed tomography (CT)) are available and can be utilized by AI technique during pregnancy. [6] In medical literature, ultrasound imaging has become popular and is used during all pregnancy trimesters. Ultrasound is crucial for making diagnoses, along with tracking fetal growth and development. Additionally, Ultrasound can provide both precise fetal anatomical information as well as high-quality photos and increased diagnostic accuracy [17], [22]. There are numerous benefits and few limitations when using Ultrasound. Acquiring the device is a very inexpensive process, particularly when compared to other instruments used on the same organs, such as MRI or Positron Emission Tomography (PET). Unlike other acquisition equipment for comparable purposes, Ultrasound scanners are portable and long-lasting. The second major benefit is that, unlike MRI and CT, the Ultrasound machine does not pose any health concerns for pregnant women as the produced signals are entirely safe for both the mother and the fetus [23]. Although the literature exploring the benefits of utilizing AI technologies for Ultrasound imaging diagnostics in prenatal care has grown, more research is needed to understand the

different roles A.I. can have in diagnostic prenatal care using ultrasound images.

1.2 Research Objective

Previous reviews on Ultrasound medical images for pregnant women using AI techniques has not been thoroughly conducted. Early reviews have attempted to summarize the use of AI in the prenatal period [22], [24]–[32]. However, these reviews are not comprehensive because they only target specific issues such as fetal cardiac function [24], Down syndrome [25], and the fetal central nervous system [26]. Similarly, other reviews have not focused on AI techniques and Ultrasound image as the primary intervention [27]–[29]. Two reviews covered the use of general AI techniques utilized in the prenatal period through Ultrasound. However, they did not focus on fetal as the primary population in their review [22], [30]. Another systematic review [31] addressed AI classification technologies for fetal health, but it only targeted cardiocography disease. Other review [32] they introduced various areas of medical AI research including obstetrics but the main focus on US imaging in general. Therefore, a comprehensive survey is necessary to understand the role of AI technologies for the entire prenatal care period using Ultrasound images. This work will be the first comprehensive study that systematically reviews how AI techniques can assist during pregnancy screenings of fetal development and improve fetus growth monitoring. In this survey we aim to (a) Describe the application of AI techniques on different fetal spatial ultrasound dimensions (b) Discuss how different methodologies are used; classification, segmentation, object-detection, regression, and reinforcement learning, (c) Highlight the dataset acquisition and availability (d) Identify practical and research Implications and gaps for future research.

2. Methods

2.1 Overview

We conducted a survey using method of systematic reviews as reported by Joanna Briggs Institute for systematic reviews [33]. The findings are reported in accordance with the Preferred Reporting Items for Systematic Reviews and Meta-Analyses (PRISMA) [34].

2.2 Search strategy

The bibliographic databases used in this study were PubMed, EMBASE, PsycINFO, IEEE Xplore, ACM Digital Library, ScienceDirect, and Web of Science. Google Scholar was also used as a search engine. The first 200 results were filtered from Google Scholar, which returned a significant number of papers sorted by relevancy to the search subject (20 pages). On June 22, 2021, the search began and ended on June 23, 2021. The original query was broad: we searched terms in all fields in all databases; due to the huge number of irrelevant studies while searching in Web of Science and ScienceDirect, we only searched article title, abstract, and keywords. We derived our preliminary search terms from previous works [22], [30] and identified additional terms in consultation with one digital health expert. Multimedia Appendix 1 lists the search strings used to search each bibliographic database.

2.3 Study Eligibility Criteria

Studies published in the last eleven years reporting on 'fetus' or 'fetal' were included in this survey. The population of interest was pregnant women in the first, second, and third trimesters with a specific focus on fetal development during these time periods. We included computer vision Artificial Intelligence interventions that

3.3 Identification of result themes

In Figure 1, we grouped the studies by the fetus organ that each study addresses including: 1) fetus head (n=43, 40.18%), 2) fetus body (n=31, 28.97%), 3) fetus heart (n=13, 12.14%), 4) fetus face (n=10, 9.34%), and 5) fetus abdomen (n=10, 9.34%). Each group is classified by sub-group as detailed in Figure 3. In addition, most of the studies used 2D US (n=88, 82.24%) and 3D/4D US were rare and reported only in (n=19, 17.75%). AI tasks are grouped based on the most common use. We found that classification was used in (n=42, 39.25%), segmentation was used in (n=31, 28.97%), both classification and segmentation were used together in (n=16, 14.95%), object-detection, regression, and reinforcement learning were seen as miscellaneous in (n=18, 16.82%).

3.4 Definition of result themes

3.4.1 Ultrasound imaging modalities

There was a total of (n=88, 82.24%) studies that utilized 2D US images. therefore, here is a brief about what's the 2D Ultrasound. Sound waves are used in all ultrasounds to produce an image. The conventional ultrasound picture of a growing fetus is a 2D image. The fetus's internal organs may be seen with a 2D ultrasound, which provides outlines and flat-looking pictures. 2D ultrasounds have been widely available for a long time and have a very good safety record. These devices do not pose the same dangers as X-rays because they employ non-ionizing rather than ionizing radiation [22]. Ultrasounds are typically conducted at least once throughout pregnancy, most often between 18 and 22 weeks in the second trimester [37]. This examination, also known as a level two ultrasound or anatomy scan, is performed to monitor fetus's development. Ultrasounds may be used to examine a variety of things during pregnancy, including: 1) how the fetus is developing; 2) the gestational age of the fetus; 3) any abnormalities within the uterus, ovaries, cervix, or placenta; 4) The number of fetuses you're carrying; 5) Any difficulties the fetus may be experiencing; 6) the fetus's heart rate; 7) fetal growth and location in the uterus, 8) amniotic fluid level, 9) sex assignment, 10) signs of congenital defects, and 11) signs of Down syndrome [38], [39].

There was a total of (n=18, 16.8%) studies that utilized 3D. Therefore, here is a brief about what's the 3D Ultrasound. Observing three-dimensional (3D) ultrasound images has increasingly grown in recent years. Although 3D ultrasounds may be beneficial in identifying facial or skeletal abnormalities [40], 2D ultrasounds are commonly utilized in medical settings because they can clearly reveal the interior organs of a growing fetus. The picture of a 3D ultrasound is created by putting together several 2D photos obtained from various angles. Many parents like 3D photos because they believe they can see their baby's face more clearly than they can with flat 2D images.

Despite this, the Food and Drug Administration (FDA) does not recommend using a 3D ultrasound for entertainment purposes [41]. The "as low as reasonably attainable" (ALARA) approach directs ultrasound technologists to be used solely in a clinical setting in order to reduce exposure to heat and radiation [42]. While ultrasound is generally thought to be harmless, there is insufficient data to determine what long-term exposure to ultrasound may do to a fetus or a pregnant woman. There is no way of knowing how long a session will take or if the ultrasound equipment will work correctly in non-clinical situations such as places that give "keepsake" photos [43].

4D ultrasound is identical to a 3D ultrasound, but the image it creates is updated constantly – comparable to a moving image. This sort of ultrasound is usually performed for fun rather than for medical concerns. As previously

mentioned, because ultrasound is medical equipment that should only be used for medical purposes [44], the FDA does

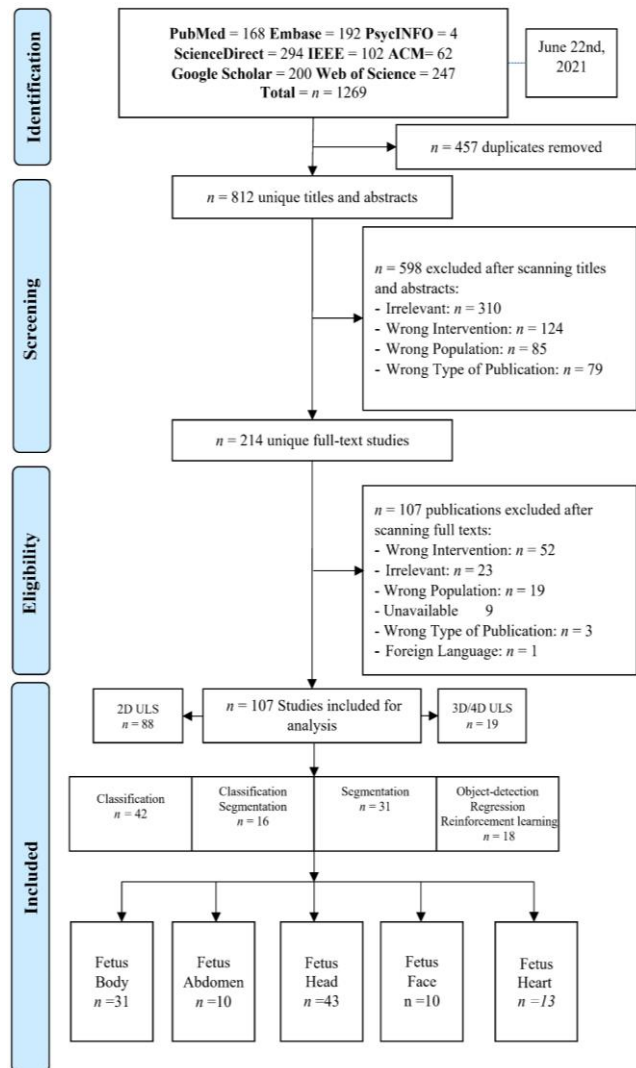


Figure 1. PRISMA diagram showing our literature search inclusion process.

not advocate getting ultrasounds for enjoyment or bonding purposes. Unless their doctor or midwife has recommended it as part of prenatal care, pregnant patients should avoid non-medical locations that provide ultrasounds[43]. Though there's no proven risk but both 3D and 4D ultrasounds employ higher-than-normal amounts of ultrasound energy and sessions are longer compared to 2D which may have fetal adverse effects[45], [46].

3.4.2 AI image processing task

There was a total of (n=42, 39.25%) studies that utilized classification, which is the process of assigning one or more labels to an image, and it is one of the most fundamental problems concerning accurate computer vision and pattern recognition. It has many applications, including image and video retrieval, video surveillance, web content analysis, human-computer interaction, and biometrics. Feature coding is an important part of image classification, and several coding methods have been developed in recent years. In general, image classification entails extracting picture characteristics before classifying them. As a result, the main aspect of utilizing image classification is understanding how to extract and evaluate image characteristics [47].

There was a total of (n=31, 28.97%) studies that utilized

segmentation, which one of the most complex task in medical image processing, that distinguishing the pixels of organs or lesions from background medical images such as CT or MRI scans. A number of researchers have suggested different automatic segmentation methods by using existing technology[48]. Previously, traditional techniques like edge detection filters and mathematical algorithms were used to construct earlier systems [49]. After this, machine learning techniques for extracting hand-crafted characteristics were the dominating method for a substantial time period. The main issue for creating such a system has always been designing and extracting these characteristics, and the complexity of these methods have been seen as a substantial barrier to deployment. In the 2000's, deep learning methods began to grow in popularity because of advancements in technology as this method had significantly better skills in image processing jobs. Deep learning methods have emerged as a top choice for image segmentation, particularly medical image segmentation, due to their promising capabilities [50]. There was a total of (n=12, 11.21%) studies that utilized object detection techniques, which is the process of locating and classifying items. A detection method is used in biomedical images to determine the regions where the patient's lesions are situated as box coordinates. There are two kinds of deep learning-based object detection. These region proposal-based algorithms are one example. Using a selective search technique, this method extracts different kinds of patches from input images. After that, the trained model determines if each patch contains numerous items and classifies them according to their region of interest (ROI). In particular, the region proposal network, was created to speed up the detection process.

Object identification in the other methods is done using the regression-based algorithm as a one-stage network. These methods use image pixels to directly identify and detect bounding box coordinates and class probabilities within entire images [6].

There was a total of (n=2, 1.8%) studies that utilized Reinforcement Learning (RL), the concept behind RL is that an artificial agent learns by interacting with its surroundings. It enables agents to autonomously identify the best behavior to exhibit in each situation to optimize performance on specified metrics. The basic concept underlying reinforcement learning is made up of many components. The RL agent is the process's decision-maker, and it tries to perform an action that has been recognized by the environment. Depending on the activity performed, the agent receives a reward or penalty from its surroundings. Exploration and exploitation are used by RL agents to determine which activities provide the most rewards. In addition, the agent obtains information about the condition of the environment [51]. For medical image analysis applications, RL provides a powerful framework. RL has been effectively utilized in a variety of applications, including landmark localization, object detection, and registration using image-based parameter inference. RL has also been shown to be a viable option for handling complex optimization problems such as parameter tuning, augmentation strategy selection, and neural architecture search. Existing RL applications for medical imaging can be split into three categories: parametric medical image analysis, medical image optimization, and numerous miscellaneous applications [52].

3.5 Description of Included Studies

As shown in Table 3, more than half of the studies (n= 53, 49.53%) were obtained from journal articles, while the other half were found in conference proceedings (n= 43, 40.18%) and book chapters (n=11, 10.28%). Studies were published between 2010 and 2021. The majority of studies were published in 2020 (n=30, 28.03%), followed by 2021 (n=19,

17.75%), 2019 (n=14, 13.08%), 2018 (n=11, 10.28), 2014 (n=9, 8.41%), 2017 (n=6, 5.60%), 2015 (n=6, 5.60%), 2016 (n=4, 3.73%), 2013 (n=3, 2.80%), 2011 (n=3, 2.80%), 2012 (n=1, 0.93%), and 2010 (n=1, 0.93%). In regard to studies examining fetal organs, fetus skull localization and measurement was reported on in (n=25, 23.36%) studies, followed by fetal part structures (n=13, 12.14%) and brain standard plane in (n=13, 12.14%) studies. Abdominal anatomical landmarks were reported in (n=10, 9.34%) studies. Additionally, fetus body anatomical structures were reported in (n=8, 7.47%) studies. Heart disease was reported on in (n=7, 6.54%) studies. Growth disease (n=6, 5.60%) and brain disease were also reported in (n=5, 4.67%) studies. The view of heart chambers was reported on in (n=6, 5.60%) studies. Fetal facial standard planes were reported in (n=5, 4.67%) studies. Gestational age (n=3, 2.80%) and face anatomical landmarks were reported on in (n=3, 2.80%) studies. Facial expressions were reported on in (n=2, 1.86%) studies, and gender identification was reported on only in (n=1, 0.93%) study. In addition, most of the studies were conducted in China (n=41, 38.31%), followed by the UK (n=25, 23.36%), and India (n=14, 13.08%). Surprisingly, some institutes mainly focused on this field and contributed high number of studies. For example, many (n=20, 18.69%) studies were conducted at the University of Oxford, UK and several (n=13, 12.14%) were conducted in Shenzhen University, China.

3.6 Organization of the survey findings

The survey is organized as shown in Figure 3. We divided AI for Fetal US medical image into five parts (Section 4), which classify fetus research by organs. In the US image, each group was divided into sub-sections based on recognized characteristics or target illnesses. This survey discusses how different tasks are used; classification, segmentation, object-detection, regression, and reinforcement learning. We discuss the leverage of public dataset in Section 5 and compared similar work depending on the fetal organ, as shown in Section 4. We also divided the discussion (Section 6) into two subsections: principle findings, and practical and scientific implications. Lastly, we highlighted research gaps and future work in Section 7.

Table 3. Characteristics of the included studies (n=107).

Characteristics	Number of studies (n, %)
Type of publication	
Journal article	(53, 49.53)
Conference proceedings	(43, 40.18)
Book chapter	(11, 10.28)
Year of publication	
2021	(19, 17.75)
2020	(30, 28.03)
2019	(14, 13.08)
2018	(11, 10.28)
2017	(6, 5.60)
2016	(4, 3.73)
2015	(6, 5.60)
2014	(9, 8.41)
2013	(3, 2.80)
2012	(1, 0.93)
2011	(3, 2.80)
2010	(1, 0.93)
Fetal Organ	
Fetus Body	(31, 28.97)
Fetal part structures	(13, 12.14)
Anatomical structures	(8, 7.47)
Growth disease	(6, 5.60)
Gestational age	(3, 2.80)
Gender	(1, 0.93)
Fetus Head	(43, 40.18)
Skull localization and measurement	(25, 23.36)
Brain standard plane	(13, 12.14)
Brain disease	(5, 4.67)
Fetus Face	(10, 9.34)
Fetal facial standard planes	(5, 4.67)
Face anatomical landmarks	(3, 2.80)
Facial expressions	(2, 1.86)
Fetus Heart	(13, 12.14)
Heart disease	(7, 6.54)
Heart chambers view	(6, 5.60)
Fetus Abdomen	(10, 9.34)
Abdominal anatomical landmarks	(10, 9.34)
Publication Country and top institute	
China	(41, 38.31)
Shenzhen University	(13, 12.14)
Beihang University	(5, 4.67)
Chinese University of Hong Kong	(4, 3.73)
Hebei University of Technology	(2, 1.86)
Fudan University	(2, 1.86)
Shanghai Jiao Tong University	(2, 1.86)
South China University of Technology	(2, 1.86)
Other institutes	(11, 10.28)
UK	(25, 23.36)
University of Oxford	(20, 18.69)
Imperial College London	(4, 3.73)
King's College, London	(1, 0.93)
India	(14, 13.08)
Japan	(4, 3.73)
Indonesia	(4, 3.73)
USA	(3, 2.80)
South Korea	(3, 2.80)
Iran	(3, 2.80)
Australia	(1, 0.93)
Canada	(1, 0.93)
Mexico	(1, 0.93)
France	(1, 0.93)
Italy	(1, 0.93)
Tunisia	(1, 0.93)
Spain	(1, 0.93)
Iraq	(1, 0.93)
Brazil	(1, 0.93)
Malaysia	(1, 0.93)

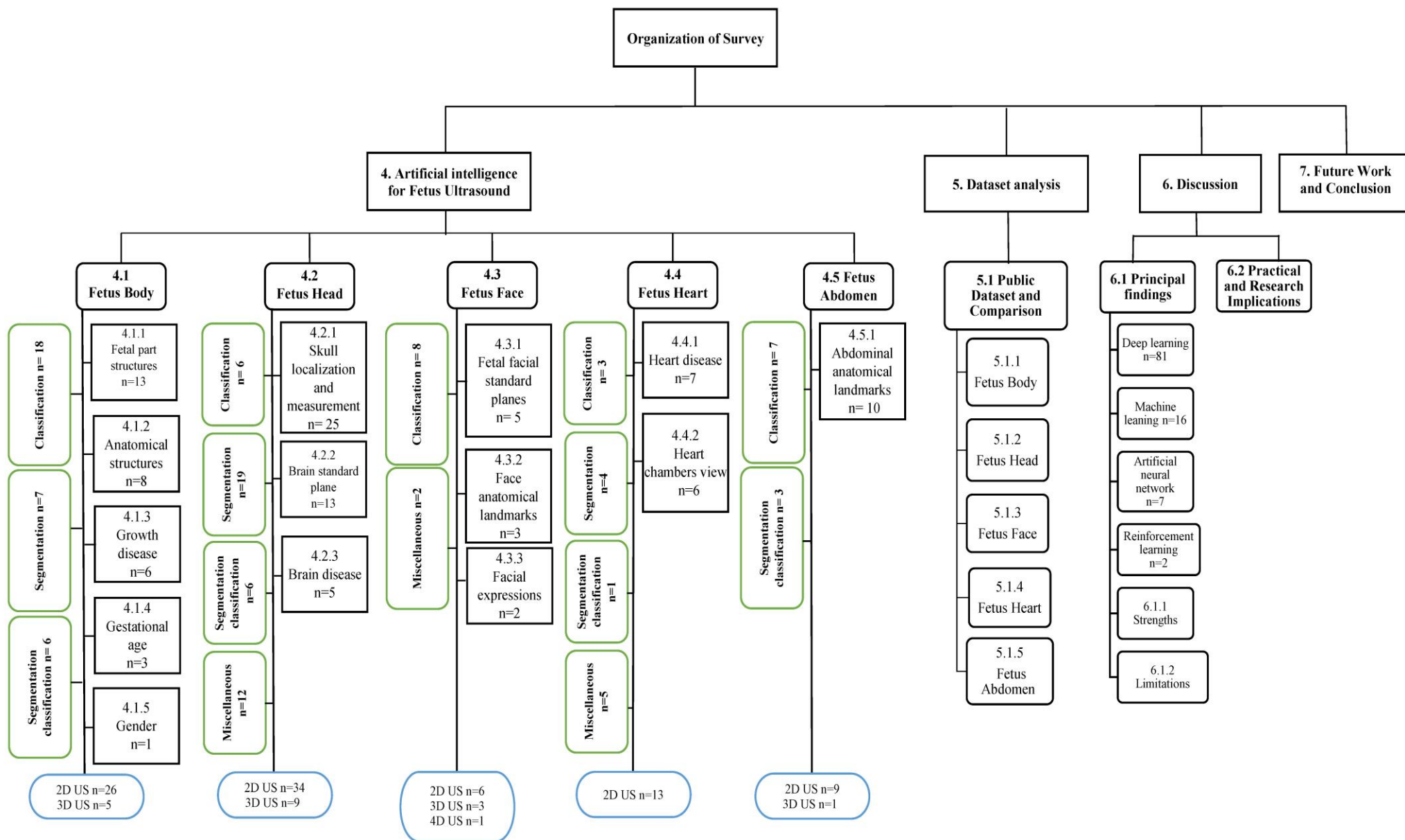


Figure 3. Organization of this survey paper

4. Artificial intelligence for fetus Ultrasound

4.1 Fetus Body

As shown in Table 3, the overall purpose of several (n= 31, 28.97%) studies was to identify general characters of the fetus (e.g., gestational age, gender) or diseases such as Intrauterine Growth Restriction (IUGR). In addition, most of the studies aimed to identify the fetus itself in the uterus or fetus part structure during different trimesters. The first trimester is from week 1 to the end of week 12. The second trimester is from week 13 to the end of week 26, and the third trimester is from week 27 to the end of the pregnancy. We also report on a performance comparison between the various techniques for each fetus body group including objective, backbone methods, optimization, fetal age, best obtained result, and observations (see Table 5).

4.1.1 Fetal Part Structures

- **Classification**

For identification and localization of fetal part structure, image classification was widely used in (n= 9, 8.41%) studies. Only 2D US images were utilized for classification purposes. Studies [53]–[55] used a classification task to identify and locate fetal skull, heart, and abdomen from 2D US images in the second trimester. Besides that, in [56], classification was used to locate the exact abdominal circumference plane (ACP), and in [57], more results were obtained by locating head circumference plane (HCP), the abdominal circumference plane (ACP), and the femur length plane (FLP). Furthermore, in studies [58]–[60] researching the second and third trimester, multi-classes were used to identify and locate various parts including fetal abdominal standard plane (FASP); 2) fetal face axial standard plane (FFASP); and 3) fetal four-chamber view standard plane (FFVSP) of heart. Study [61] located the mother's cervix in addition to abdomen, brain, femur, and thorax.

- **Segmentation**

Image segmentation task was used in (n=3, 2.80%) studies for the purpose of fetal part structure identification. 2D US imaging [62] was used to segment neonatal hip bone including seven key structures: 1) chondro-osseous border (CB), 2) femoral head (FH), 3) synovial fold (SF), 4) joint capsule & perichondrium (JCP), 5) labrum (La), 6) cartilaginous roof (CR), and 7) bony roof (BR). Only one study in [63] provided segmentation model that able to segment fetus kidney using 3D US in the third trimester. Segmentation was used to locate fetal head, femur, and humerus using 2D US as seen in [64].

- **Classification and segmentation**

In [65], whole fetal segmentation followed by classification tasks were used to locate the head, abdomen (in sagittal view), and limbs (in axial view) using 3D US images taken in the first trimester.

4.1.2 Anatomical Part Structures

- **Classification**

For identification and localization of anatomical structures, image classification was used in (n= 4, 3.73%) studies. Only one study [66] used 3D US images and other studies used 2D US [67]–[69]. In [66], the whole fetus was localized in the sagittal plane and classifier was then applied to the axial images to localize one of three classes (head, body and non-fetal) during the second trimester. Multi-classification methods were utilized in [67] to localize head, spine, thorax, abdomen, limbs, and placenta in the third trimester. Moreover, binary classification was used in [68] to identify abdomen versus non-abdomen. In [69], classification method was used to detection and

measurement nuchal translucency (NT) in the beginning of second trimester. Moreover, monitoring NT combined with maternal age can provide effective insight of screening Down syndrome.

- **Segmentation**

An image segmentation task was used in (n= 4, 3.73%) studies for the purpose of fetal image segmentation was target task anatomical structures identification. In [70], [71], 3D US were utilized to segment fetus, gestational sac amniotic fluid, and placenta in the beginning of second trimester. However, in [72], 2D US was used to segment amniotic fluid and the fetus in the late trimester. Finally, 2D US in [73] was utilized to segment and measure nuchal translucency (NT) in the first trimester of pregnancy.

4.1.3 Growth disease diagnosis

- **Classification**

For diagnosis of fetal growth, disease image classification was conducted in (n= 4, 3.73%) studies using 2D US. In [74] binary classification was used for early diagnosis of Intrauterine Growth Restriction (IUGR) at the third trimester of pregnancy. The features considered to determine a diagnosis of IUGR are gestational age (GA), biparietal diameter (BPD), abdominal circumference (AC), head circumference (HC), and femur length (FL). Additionally, binary-classification was used in the second trimester of pregnancy to identify normal vs abnormal fetus growth as seen in [75]. In [76], binary-classification is used to identify the normal growth of the ovum by distinguishing Blighted Ovum from healthy Ovum. Lastly, the binary classification was used to distinguish between healthy fetuses and those with Down syndrome [77].

- **Classification and segmentation**

For diagnosis of fetal growth disease, image classification along with segmentation were used in (n= 2, 1.86%) studies using 2D US. In [78], [79], segmentation of the region of interest (ROI), followed by classification to diagnosis (IUGR) (normal vs abnormal) were carried out. This was done by using US Images taken in both second and third trimester of pregnancy. This classification relied on the measurement of the following: 1) Fetal abdominal circumference (AC), 2) Head circumference (HC), 3) Biparietal diameter (BPD), 4) Femur length.

4.1.4 Gestational age (GA) estimation

- **Classification and segmentation**

Both classification as well as segmentation tasks were used to estimate GA in (n=3, 2.80%) studies using 2D US taken in the second and third trimester of pregnancy. In [80], the trans-cerebellar diameter (TCD) measurement was used to estimate GA in week. The TC plane frames are extracted from the US images using classification. Segmentation then localizes the TC structure and performs automated TCD estimation, from which the GA can thereafter be estimated via an equation. In [81], 2D US was used to estimate GA based on region of fetal lung in the second and third trimester. In the first stage, the segmentation is to learn the recognition of fetal lung region in the ultrasound images. Classification is also used to accurately estimate the gestational age from the fetal lung region of ultrasound images. Several fetal structures were used to estimate GA in [82], which focused on the second trimester. In this study, 2D US images were classified into four categories: head (BPD and HC), abdomen (AC), femur (FL), and fetus (crown-rump length: CRL). Then, the regions of interest (i.e., head, abdomen, and femur) were segmented and the results of biometry measurements were used to estimate GA.

4.1.5 Gender identification

- **Classification**

Binary-classification was used in [83] to identify the

gender of the fetus. Image preprocessing, image segmentation, and feature extraction (shape description) were used to obtain the value of the feature extraction and gender classification. This task is categorized as classification because a segmentation task is not clearly defined.

4.2 Fetus Head

As shown in Table 3, the primary purpose of (n= 43, 40.18%) studies is to identify and localize fetus skull (e.g., head circumference), brain standard planes (e.g., Lateral sulcus (LS), thalamus (T), choroid plexus (CP), cavum septi pellucidi (CSP)) or brain diseases (e.g., hydrocephalus (premature GA), ventriculomegaly, central nervous system (CNS) malformations)). The following subsection discusses each category based on the implemented task. Table 6 presents comparison between the various techniques for each fetus head group including objective, backbone methods, optimization, fetal age, best obtained result, and observations. studies for each group under the fetus head category and provides an overview of methodology and observations.

4.2.1 Skull localization and measurement

• Classification

Classification tasks for skull localization and head circumference are rarely used, as seen only in (n=3, 2.80%) studies. Studies [84], [85] used classification to localize the region of interest (ROI) and identify the fetus head based on 2D US taken in first and second trimester respectively. 3D US taken in first trimester were used to detect a fetal head in one study [86].

• Segmentation

Skull localization and head circumference (HC) in most of the studies (n=16, 14.81%) used segmentation task. 2D US was used in 16 studies and one study used 3D US. Various network architecture were used to segment and locate skull, then perform head circumference as seen in [87]–[99]. Besides identifying HC, in [100] segmentation was also used to find fetal biparietal diameter (BPD). Further investigation shows that the work completed in [101] was the first investigation about whole fetal head segmentation in 3D US. The segmentation network for skull localization in [91] was tested to identify a view of the four heart chambers on different datasets.

• Miscellaneous

Along with segmentation, another method was used to locate and identify the fetus skull in (n=6, 5.60%) studies. As seen in [102], regression was used along with segmentation to identify HC, BPD, and occipitofrontal diameter (OFD). Besides this, in [103], neural network was used to train the saliency predictor and predict saliency maps to measure HC and identify the alignment of both trans ventricular (TV) as well as trans cerebellar (TC). In addition, an object detection task was used along with segmentation in [104] to locate the fetal head at the end of the first trimester. In [105], object detection was used for head localization and centering and regression to delineate the HC accurately. In [106], classification and segmentation tasks were used by utilizing a multi-Task network to identify head composition.

4.2.2 Brain standard plane

• Classification

The classification was used in (n=2, 1.86%) studies to identify the brain standard plane, and both studies used 2D US images taken in the second and third trimesters. In [107], [108], two different classification network architectures were used to identify six fetal brain standard planes. These architectures include horizontal transverse section of the thalamus, horizontal transverse section of the lateral ventricle, transverse section of the cerebellum, midsagittal plane, paracentral sagittal section, and coronal section of the

anterior horn of the lateral ventricles.

• Segmentation

The segmentation task was used in (n=3, 2.80%) studies to identify the brain standard plane. Each of these studies used 2D US images. In [109], 2D US images taken in the second trimester were used to segment fetal cerebellum structure. In addition, in [110], 2D US images taken in the third trimester were used to segment fetal Middle Cerebral Artery (MCA). Authors in [111] utilized 3D US images in the second trimester to formulate the segmentation as a classification problem to identify the following brain planes; background, Choroid Plexus (CP), Lateral Posterior Ventricle Cavity (PVC), the Cavum Septum Pellucidi (CSP), and Cerebellum (CER).

• Classification and segmentation

Classification with segmentation is employed in (n=3, 2.80%) studies to identify the brain standard plane. These studies all used 3D US images. In [112], both tasks were used to identify brain alignment based on skull boundaries and then head segmentation, eye localization, and prediction of brain orientation in the second and third trimesters. Moreover, in [113], segmentation followed by a classification task was used to detect cavum septi pellucidi (CSP), thalami (Tha), lateral ventricles (LV), cerebellum (CE), and cisterna magna (CM) in the second trimester. Segmentation and classification are employed by 3D US in [114] to identify the skull, midsagittal plane, and orbits of the eyes in the second trimester of pregnancy.

• Miscellaneous

For brain standard planes identification in (n=5, 4.62%), methods different than previously mentioned were used, including; segmentation with object detection, object detection, classification with object detection, and Reinforcement Learning (RL). As seen in [115], the RL-based technique was employed for the first time on 3D US images to localize standard brain planes, including trans-thalamic (TT) and trans-cerebellar (TC) in the second and third trimesters. RL is used in [116] to localize the following: mid-sagittal (S), transverse (T), and coronal (C) planes in volumes and trans-thalamic (TT), trans-ventricular (TV), and trans-cerebellar (TC)). Object detection architecture is utilized on 2D US images in [117] to localize the trans-thalamic plane in the second trimester of pregnancy, including lateral sulcus (LS), thalamus (T), choroid plexus (CP), cavum septi pellucid (CSP), and third ventricle (TV). In [118], classification with object detection was used to detect Lateral sulcus (LS), thalamus (T), choroid plexus (CP), cavum septi pellucidi (CSP), third ventricle (TV), brain midline (BM). In contrast, [119] used classification with object detection to localize cavum septum pellucidum (CSP) and ambient cistern (AC) and cerebellum), as well as to measure head circumference (HC) and biparietal diameter (BPD).

4.2.3 Brain disease

• Classification

The Binary-classification technique utilized 2D US images taken in the second trimester as seen in [120] to detect hydrocephalus disease using premature GA.

• Classification and segmentation

Studies [121], [122] both used 2D US images taken in the second and third trimesters to segment craniocerebral and identify abnormalities or specific diseases. As seen in [121], central nervous system (CNS) malformations were detected using binary classification. Moreover, in [122], multiclassification was used to identify the following problems: TV planes contained occurrences of ventriculomegaly and hydrocephalus, and TC planes contained occurrences of Blake pouch cyst (BPC).

• Miscellaneous

In [123], [124] different methods were used to detect ventriculomegaly disease based on 2D US images taken in the second trimester. In study [123], object detection and regression first identify fetal brain ultrasound images from standard axial planes as normal or abnormal. Second regression was then used to find the lateral ventricular regions of images with big lateral ventricular width. Then, the width was anticipated with a modest error based on these regions. Furthermore, [124] was the first study to propose an object-detection-based automatic measurement approach for fetal lateral ventricles (LVs) based on 2D US images. The approach can both distinguish and locate the fetal LV automatically as well as measure the LV's scope quickly and accurately.

4.3 Fetus Face

As shown in Table 3, the primary purpose of (n= 10, 9.34%) studies was to identify and localize fetus face features such as the fetal facial standard plane (FFSP) (i.e., axial, coronal, and sagittal plane), face anatomical landmarks (e.g., Nasal Bone), and facial expressions (i.e., sad, happy). The following subsection discusses each category based on the implemented task. Table 7 presents comparison between the various techniques for each fetus face group including objective, backbone methods, optimization, fetal age, best obtained result, and observations.

4.3.1 Fetal facial standard plane (FFSP)

- **Classification**

Classification was used to classify the FFSP using 2D US Images as seen in (n=5, 4.67%). Using 2D US images that taken in the second and third trimesters, four studies [125]–[128] identify ocular axial planes (OAP), the median sagittal planes (MSP), and the nasolabial coronal planes (NCP). In addition, authors in [129] were able to identify the FFSP using 2D US images taken in the second trimester.

4.3.2 Face anatomical landmarks

- **Miscellaneous**

Different methods were used to identify face anatomical landmarks in (n=3, 2.80) studies. In [130], 3D US images taken in the second and third trimesters were segmented to identify background, face mask (excluding facial structures), eyes, nose, and lips. In another study the object detection method was used on 3D US images in [131] to detect the left fetal eye, middle eyebrow, right eye, nose, and chin. Furthermore, classification used 2D US images taken in the first and second trimesters to detect the nasal bone. This was done to enhance the detection rate of Down syndrome, as seen in [132].

4.3.3 Facial expressions

- **Classification**

For the first time, 4D US images were utilized using the multi-classification method to identify fetus facial expression into Sad, Normal, and Happy as seen in [133]. Study [134] used 2D US images in the second and third trimesters to classify fetal facial expression into eye blinking, mouthing without any expression, scowling, and yawning.

4.4 Fetus Heart

As shown in Table 3, the primary purpose of (n= 13, 14.04%) studies is to identify and localize fetus heart diseases and the fetus heart chambers view. The following subsection discusses each category based on the implemented task. Table 8 presents comparison between the various techniques for each fetus heart group including objective, backbone methods, optimization, fetal age, best obtained result, and observations.

4.4.1 Heart disease

- **Classification**

Two studies used classification methods to identify heart diseases based on 2D US images taken in the second trimester. In [135], binary-classification task was utilized to identify Down syndrome vs normal fetuses based on

identifying the echogenic intracardiac foci (EIF). Furthermore, in [136], binary-classification task was utilized to detect hypoplastic left heart syndrome (HLHS) vs healthy cases based on the four-chamber heart (4CH), left ventricular outflow tract (LVOT), and right ventricular outflow tract (RVOT).

- **Segmentation**

2D US images were utilized by multi-class segmentation to identify heart disease, including: left heart syndrome (HLHS), total anomalous pulmonary venous connection (TAPVC), pulmonary atresia with intact ventricular septum (PA/IVS), endocardial cushion defect (ECD), fetal cardiac rhabdomyoma (FCR), and Ebstein's anomaly (EA) [137].

- **Classification and segmentation**

Classification and segmentation are used to detect congenital heart disease (CHD) based on 2D US images taken in the second trimester [138]. Cases were classified into normal hearts vs CHD. This classification was orchestrated by identifying five views of the heart in fetal CHD screening, including three-vessel trachea (3VT), three-vessel view (3VV), left-ventricular outflow tract (LVOT), axial four chambers (A4C), and abdomen (ABDO).

- **Miscellaneous**

To identify heart disease, various methods were proposed based on the capabilities of 2D US images. Classification with object detection were utilized in [139], [140]. Fetal congenital heart disease (FHD) can be detected in the second and third trimesters based on how quickly the fetus grows between gestational weeks, and how the shape of the Four Chambers heart changes over time [139]. Furthermore, classification with object detection was used to detect cardiac substructures and structural abnormalities in the second and third trimesters [140]. Lastly, segmentation with object detection was used to locate the ventricular septum in 2D US images in the second trimester, as seen in [141].

4.4.2 Heart chambers view

- **Classification**

2D US images taken in the second and third trimesters were utilized in [142] to propose a classification task utilized to localize the four chambers (4C), the left ventricular outflow tract (LVOT), the three vessels (3V), and the background (BG).

- **Segmentation**

Segmentation was used in (n=3, 2.80%) studies based on 2D US images. In two studies [143], [144], seven critical anatomical structures in the apical four-chamber (A4C) view were segmented, including: left atrium (LA), right atrium (RA), left ventricle (LV), right ventricle (RV), descending aorta (DAO), epicardium (EP) and thorax. In another study [145], segmentation was used to locate four-chamber views (4C), left ventricular outflow tract view (LVOT), and three-vessel view (3V) in the second and third trimesters.

- **Miscellaneous**

2D US images were used in (n=2, 1.86) studies, and both studies utilized classification with object detection. In the second trimester [146], the first classification conducted was the cardiac four-chamber plane (CFP) into non-CFPs and CFPs (i.e., apical, bottom, and parasternal CFPs). The second task was to then classify the CFPs in terms of the zoom and gain of 2D US images. In addition, object detection was utilized to detect anatomical structures in the CFPs, including left atrial pulmonary vein angle (PVA), apex cordis and moderator band (ACMB), and multiple ribs (MRs). In [147], object detection was used in the second and third trimesters to extract attention regions for improving classification performance and determining the four-chamber view, including detection of end-systolic (ES) and end-diastolic (ED).

4.5 Fetus Abdomen

As shown in Table 3, the primary purpose of (n= 10,

10.8%) studies was to identify and localize the fetus's abdomen, including abdominal anatomical landmarks (i.e., stomach bubble (SB), umbilical vein (UV), and spine (SP)). The following subsection discusses this category based on the implemented task. Table 9 presents comparison between the various techniques for each fetus abdomen including objective, backbone methods, optimization, fetal age, best obtained result, and observations.

4.5.1 Abdominal anatomical landmarks

- **Classification**

Classification task was used in (n=7, 6.54%) studies to localize abdominal anatomical landmarks. 2D US images were used in seven studies [148]–[153] and 3D US images in only one study [154]. In [148], [150], [152], [154], various classifiers were utilized to localize stomach bubble (SB) and umbilical vein (UV), in the first and second trimester as seen in [148], [154], and in the second and third trimesters as seen in [150], [152]. Furthermore, works in [149], [151], [153] located the spine (SP) besides SB and UV on the same trimesters.

- **Classification and segmentation**

2D US images taken within random trimesters were used in [155], [156]. In [155], SB, UV, and AF were localized. Further, abdominal circumference (AC), spine position, and bone regions were estimated. In [156], 2D US images were classified into normal vs abnormal fetuses based on the fetus images such as AF, SB, UV, and SA. Study [157] located SB and the portal section from the UV, and observed amniotic fluid (AF) in the second and third trimesters.

5. Dataset Analysis

5.1 Public dataset

5.1.1 Fetus Body

In this area, ethical and legal concerns presented the most barriers to comprehensive research. Therefore, datasets were not available to the research community. For example, in this research, studies discussed how the fetal body contains five subsections (fetal part structure, anatomical structure, growth disease, gestational age, and gender identification). Out of the available studies (n=31, 28.9%), one dataset was intended to be available online in [55] related to identifying fetal part structure. Unfortunately, this dataset has not yet been released by the author. The only public dataset that was available online for fetal structure classification was released by Burgos-Artiz et al. [61], the dataset is a total of 12499 2D fetal ultrasound images, including brain 143, Trans-cerebellum 714, Trans-thalamic 1638, Trans-ventricular 597, abdomen 711, cervix 1626, femur 1040, thorax 1718, and 4213 are unclassified fetal image. Acquiring a high volume of the dataset was also challenging in most of the studies; therefore, multi-data augmentation in (n=11, 10.2%) studies [54], [56], [61], [63], [65], [70], [72], [76], [80] has been observed. These augmented images were employed to boost classification and segmentation performance. SimpleITK library [158] was used for augmentation in [63]. Due to limited data sample in addition to augmentation, k-fold cross-validation method was utilized in (n=8, 7.4%) studies [54], [55], [57], [64], [66], [69], [74], [83]. These cross-validation methods are also used to resolve issues such as overfitting and bias in dataset selection. Only one software named ITK-SNAP [159] was reported in [63] to segment structures in 3D images.

5.1.2 Fetus Head

This section contains three subsections (skull localization, brain standard planes, and brain disease). Total studies (n=43, 40.18%), but we only found one online public dataset called HC18 grand challenge [160]. This dataset was used in (n=13, 12.14%) studies [87]–[89], [91], [92], [95]–[98], [102], [104], [105], [161]. This dataset contains 2D US images collected from 551 pregnant women at different pregnancy trimesters. There were 999 images in the training set and 335 for testing; the sonographer manually annotated the HC. Image

augmentation was applied in (n=9, 8.41%) studies [87], [89], [92], [96], [98], [102], [104], [105], [161], and cross-validation was employed in [161]. Table 4 highlights the best result achieved despite the challenges of recording the outcomes of the selected studies.

Table 4. Compared between studies that utilized the HC18 dataset

Study	DSC	HD	DF	ADF
[87]	0.926	3.53	0.94	2.39
[88]	N/A	N/A	14.9%	N/A
[95]	0.973	1.58	N/A	N/A
[96]	0.968	N/A	N/A	N/A
[97]	0.973	N/A	N/A	2.69
[98]	0.968	1.72	1.13	2.12
[89]	0.979	1.27	0.09	1.77
[105]	0.977	1.32	0.21	1.90
[102]	0.977	0.47	N/A	2.03
[104]	0.977	1.39	1.49	2.33
[91]	0.971	3.23	N/A	N/A
[92]	0.979	N/A	N/A	N/A
[161]	N/A	N/A	N/A	N/A

DSC: Dice similarity coefficient, ACC: Accuracy, Pre: Precision, HD: Hausdorff distance, DF: Difference, ADF: Absolute Difference, IoU: Intersection over Union, mPA: mean Pixel Accuracy.

5.1.3 Fetus Face

This section contains three subsections (fetal facial standard planes, face anatomical landmarks, and facial expression). Out of these studies (n=10, 9.34%), we did not find any public dataset available online. However, within the private dataset, image augmentation was applied in (n=3, 2.8%) studies [130], [131], [134]. The k-fold cross-validation was employed in [125], [129], [130]. Lastly, 3D Slicer software [162] was used for image annotation as reported in [130].

5.1.4 Fetus Heart

This section contains two subsections (heart diseases and heart chamber view). Out of these studies (n=13, 12.14%), we did not find any public dataset available online. However, within the private dataset, the image augmentation was applied in (n=4, 3.7%) studies [137], [138], [145], [147]. The k-fold cross-validation was employed in [138], [139], [141], [144], [146].

5.1.5 Fetus Abdomen

This section contains one subsection (abdominal anatomical landmarks). Out of these studies (n=10, 9.34%), we did not find any public dataset available online. However, within the private dataset, image augmentation was applied in (n=4, 3.7%) studies [150], [153], [155], [157]. The cross-validation was not reported in any of the studies.

Table 5. Articles published using AI to improve fetus body monitoring: Objective, backbone methods, optimization, fetal age best result, and observations

Study	Objective	Backbone Methods/Framework	Optimization/ Extractor methods	Fetal age	Best Obtained Result	observations
Fetal Part Structures						
[53]	To identify the fetal skull, heart and abdomen from ultrasound images	SVM as the classifier	Gaussian Mixture Model (GMM) Fisher Vector (FV)	26 th week	Acc: 0.9890 mAP: 0.9985	1) Methodology and result are clear. 2) Dataset acquisition is clear splitting is not. 3) No data augmentation and no cross-validation. 4) Important performance metrics are missing.
[62]	To segment the seven key structures of the neonatal hip joint	Neonatal Hip Bone Segmentation Network (NHBSNet)	Feature Extraction Module Enhanced Dual Attention Module (EDAM) Two-Class Feature Fusion Module (2-Class FFM) Coordinate Convolution Output Head (CCOH)	16 to 25 weeks.	DSC: 0.8785 HD: 8.42 mm AHD: 0.32 mm	1) Multi-mechanisms were used to build the framework; the method is clear 2) Data acquisition is precise, but data splitting could be more interpreted 3) No data augmentation and no cross-validation method 4) Novel work and unique in the target area.
[64]	To segment organs head, femur, and humerus in ultrasound images using multilayer super pixel images features	Simple Linear Iterative Clustering (SLIC) Random forest	Unary pixel shape feature image moment	N/A	Head Femur Humerus Acc: 0.969 0.986 0.981 F1 : 0.531 0.456 0.357 Rec: 0.803 0.758 0.760 Spec: 0.972 0.988 0.9831	1) Methodology and results are not presented clearly. 2) Dataset is small; acquisition, and splitting are not clear. 3) No data augmentation.
[63]	To automate kidney segmentation using fully convolutional neural networks.	FCNN: U-Net & UNET++	N/A	20 to 40 weeks	DSC: 0.81 Jaccard index (JI): 0.69 HD: 8.96 mm Mean Surface Distance (MSD) 2.04 mm	1) Methodology and results are confusing but should be interpreted in a better way. 2) Dataset is very small even after augmentation; data acquisition is precise, but data splitting is not clear. 3) No cross-validation was applied. 4) First study that target fetus kidney segmentation.
[61]	To evaluate the maturity of current Deep Learning classification techniques for their application in a real maternal-fetal clinical environment	CNN DenseNet-169	N/A	18 to 40 weeks	Acc: 0.936 Error rate: 0.27	1. Methodology and results are not clear. 2. Dataset is large, data acquisition and splitting are precise. 3) No cross-validation was applied. 4) No comparison with state-of-the-art methods. 5) Missing significance performance metrics 6) Models have similar performance compared to an expert when classifying standard planes.
[57]	To uses the learnt visual attention maps to guide standard plane detection on all three standard biometry planes: ACP, HCP and FLP.	Temporal SonoEyeNet (TSEN) Temporal attention module: Convolutional LSTM Video classification module: Recurrent Neural Networks (RNNs)+	CNN feature extractor: VGG-16	N/A	Pre: 0.894 Rec: 0.851 F1 : 0.871	Many technologies were integrated to build hybrid framework, the work is very detailed, but two significant points should be considered: 1) Dataset distribution and volume was not clear 2) Paper structure and organization does not help the reader to understand
[39]	To support first trimester fetal assessment of multiple fetal anatomies including both visualization and the measurements from a single 3-D ultrasound scan	Multi-Task Fully Convolutional Network (FCN) U-Net	N/A	11 to 14 weeks	Mean Acc: 0.894 Intersection over Union (IoU): 0.76	1) clinical 3-D datasets was too small for a 3-D FCN implementation even with data augmentation. 2) Other performance metrics were not used such as F1 score and recall
[58]	To automatically classify 14 different fetal structures in 2-D fetal ultrasound images by fusing information from both cropped regions of fetal structures and the whole image	support vector machine (SVM)+ Decision fusion	Fine-tuning AlexNet CNN	18 to 20 weeks	Mean of all structure's classification Acc: 0.97 Pre: 0.76	1) Large dataset but no cross validation applied 2) paper is not organized in solid way 3) Role of SVM and Decision fusion were confusing for the reader
[59]	To automatic identification of different standard planes from US images	T-RNN framework: LSTM	Features extracted using J-CNN classifier	18 to 40 weeks	FASP FFASP FVSP Acc: 0.94 0.71 0.84 Pre: 0.94 0.73 0.89 Rec: 0.99 0.95 0.93 F1: 0.96 0.96 0.96	1) largest dataset no cross-validation applied 2) incorrect comparison with other work due to different dataset 3) T-RNN framework could be explained in a better way, such as point form
[56]	To classify abdominal fetal ultrasound video frames into standard AC planes or background.	M-SEN architecture Discriminator CNN	Generator CNN	N/A	Pre: 0.968 Rec: 0.962 F1 : 0.965	1) Dataset acquisition detailed is missing, the dataset small, and no cross-validation is applied 2) Methodology is not clear 3) Novel and effective algorithm that models sonographer visual attention.
[54]	To detect of multiple fetal structures in free-hand ultrasound	CNN Attention Gated LSTM	Class Activation Mapping (CAM)	28 to 40 weeks	mean IOU is above 0.50 Skull Average Pre: 0.94 Abdomen Average Pre: 0.93 Heart Average Pre: 0.85	1) Dataset acquisition and splitting is not apparent 2) Only precision and IOU as performance metrics
[55]	To extract features from regions inside the images where meaningful structures exist.	Guided Random Forests	Probabilistic Boosting Tree (PBT)	18 to 22 weeks	Mean Acc for all classes: 0.91	1) Dataset acquisition and splitting is not apparent 2) Only accuracy as performance metrics
[60]	To detect standard planes from US videos	T-RNN LSTM (Transferred RNN)	Spatio-Temporal Feature J-CNN	18 to 40 weeks	FASP FFASP FVSP Acc: 0.90 0.86 0.86 Pre: 0.74 0.63 0.77 Rec: 0.74 0.59 0.61 F1: 0.74 0.61 0.68	1. largest dataset no cross-validation applied 2. incorrect comparison with other work due to different dataset 3. T-RNN framework could be explained in a better way, such as point form 4. Same work in [59]
Anatomical Structures						
[70]	To propose the first and fully automatic framework in the field to simultaneously segment fetus, gestational sac and placenta,	3D FCN + RNN hierarchical deep supervision mechanism (HiDS)	BiLSTM module denoted as FB-nHiDS	10 to 14 weeks	DSC: 0.890 Coefficient Conformity: 0.749 Average Distance of Boundaries: 0.925 HD of Boundaries: 9.788 mm	1) Methodology and results are very detailed but could be interpreted in better way. 2) Dataset is very small even after augmentation, data acquisition, and splitting are precise.
[71]	To segment the placenta, amniotic fluid, and fetus.	FCNN	N/A	11 to 19 weeks	Placenta AF Fetus DSC: 0.82 0.93 0.88 HD: 16.22 10.86 16.57 Average HD: 0.85 0.13 0.22	1) Methodology and results are very detailed, but multi-model experiments confuse the reader. 2) Dataset acquisition is clear, but data splitting is not precise. 3) No cross-validation was applied, no augmentation
[72]	To segment the amniotic fluid and fetal tissues in fetal US images	The encoder-decoder network based on VGG16	N/A	22 nd weeks	Mean for all categories: Acc: 0.8099 IoU: 0.7083	1) Methodology is not explained well. 2) Dataset is very large after augmentation; data acquisition clear but splitting is not precise. 3) Cross-validation was applied. 4) Different methods were compared.
[66]	To localize the fetus and extract the best fetal biometry planes for the head and abdomen from first trimester 3D fetal US images	CNN	Structured Random Forests	11 to 13 weeks	Mean ACC: 0.769 IoU: ≥ 0.50	1) Dataset acquisition and splitting is not apparent 2) Methodology steps are confusing for the reader
[67]	To detect and localize fetal anatomical regions in 2D US images	ResNet18	Soft Proposal Layer (SP)	22 to 32 weeks	ACC: 0.912 IoU: 0.393	1) Dataset splitting is well explained but source and acquisition not clear 2) Validation is not applied
[68]	To reliably estimate abdominal circumference	CNN + Gradient Boosting Machine (GBM)	Histogram of Oriented Gradient (HoG)	15 to 40 weeks	DSC: 0.90	1) Dataset acquisition and splitting is not apparent. 2) Methodology is not organized well. 3) Validation is not applied. 4) Only DSC as performance metrics.
[69]	To detect and recognize the fetal NT based on 2D ultrasound images by using artificial neural network techniques.	Artificial Neural Network (ANN)	Multilayer Perceptron (MLP) Network Bidirectional Iterations Forward Propagations Method (BIFP)	N/A	ACC: 0.933 (56/60) Spec: 0.966 Rec: 0.900	1) Small dataset, acquisition and splitting is not apparent 2) Framework could be explained in a better way, such as point form
[73]	To detect NT region	U-Net NT Segmentation PCA NT Thickness Measurement	VGG16 NT Region Detection	4 to 12 weeks	IoU: 0.71 Detection Error (in pixel): 41.54	1) Dataset acquisition is not apparent. 2) Methodology very clear and explained in a consistent way. 3) Only IoU and error rate for evaluation

(Continued)

Table 5. Continued

Study	Objective	Backbone Methods/Framework	Optimization/ Extractor methods	Fetal age	Best Obtained Result	observations
Growth disease						
[74]	To propose the biometric measurement and classification of IUGR, using OpenGL concepts for extracting the feature values and ANN model is designed for diagnosis and classification	ANN Radial Basis Function (RBF)	OpenGL	various	ACC: 0.94 Root Mean Square Error (RMSE): 0.67	1) Methodology is not explained well. 2) Dataset is small; data acquisition and splitting is not precise. 3) Cross-validation was applied. 4) Two models were compared.
[75]	To find the region of interest (ROI) of the fetal biometric and organs region in the US image	DCNN AlexNet	N/A	16 to 27 weeks	ACC: 0.9043	1) Dataset acquisition and splitting is not apparent. 2) Validation is not applied. 3) Only accuracy as performance metrics
[78]	To detect of fetal abnormality in 2-D US images	ANN + Multilayered perceptron neural networks (MLPNN)	Gradient vector flow (GVF) Median Filtering	14 to 40 weeks	HC MSE: 0.087 AC 0.177	1) Dataset acquisition and splitting is not apparent. 2) Validation is not applied. 3) Only Mean square error as performance metrics
[79]	To develop a computer aided diagnosis and classification tool for extracting ultrasound sonographic features and classify IUGR fetuses	ANN	Two-Step Splitting Method (TSSM) for Reaction-Diffusion (RD)	various	RMSE: 0.91 to 0.94	1) Dataset acquisition and splitting is not apparent. 2) Validation is not applied. 3) Only RMSE as performance metrics
[76]	To develop an automatic classification algorithm on the US examination result using Convolutional Neural Network in Blighted	CNN	N/A	N/A	ACC: 0.60	1) Dataset acquisition is missing. 2) Insufficient dataset was used 3) Validation is not applied 4) Only accuracy as performance metrics
[77]	To proposes an intelligent system based on combination of ConvNet and PSO for Down Syndrome diagnosis.	CNN	Particle Swarm Optimization (PSO)	N/A	ACC: 0.99	1) Small dataset and dataset acquisition is not apparent. 2) Methodology could be explained in a better way 3) Only accuracy as performance metrics. 4) The idea is novel but obtained very high accuracy on small dataset is suspicious.
Gestational age (GA)						
[80]	To automatic detect and measure the trans cerebellar diameter (TCD) in the fetal brain, which enables the estimation of fetal gestational age (GA)	CNN FCN	N/A	16- to 26 weeks	ACC: 0.9789 IoU: 0.8162	1) Methodology and results are not clear. 2) Dataset is sufficient after augmentation, data acquisition and is precise. 3) No cross-validation was applied. 4) No comparison with state-of-the-art methods. 5) missing signification performance metrics
[81]	To accurately estimate the gestational age from the fetal lung region of US images.	U-NET	N/A	24 to 40 weeks	Correlation coefficient: 0.76 P-value: 0.00001	1) Dataset acquisition is detailed but the dataset small, and no cross-validation is applied 2) Missing essential performance metrics. 3) Methodology was not clear for the reader.
[82]	To classify, segment, and measure several fetal structures for the purpose of GA estimation	U-NET RESTNET	Residual UNET (RUNET)	16 th weeks	ACC: 0.93 IoU: 0.91 Mean Absolute Error: 1.89 centimeters	1) Dataset acquisition and splitting is not apparent, and no cross-validation is applied 2) Methodology steps are clear and organized
Gender identification						
[83]	To measure the accuracy of Learning Vector Quantization (LVQ) to classify the gender of the fetus in the US image"	ANN	Learning Vector Quantization (LVQ) Moment invariants	N/A	Mean Absolute Error (MAE):0.3889. Rec: 0.611 Pre: 0.58 F1: 0.556"	1) Methodology is not clear, but obtained result is clearly explained. 2) Dataset is very small; data acquisition and splitting are not precise. 3) Cross-validation was applied, no augmentation. 4) Different models were compared. 5) Novel work by identifying gender in early stage of pregnancy.

Table 6. Articles published using AI to improve fetus head monitoring: Objective, backbone methods, optimization, fetal age best result, and observations

Study	Objective	Backbone Methods/Framework	Optimization/ Extractor methods	Fetal age	Best Obtained Result	observations	
Skull localization and measurement							
[87]	To localize the fetal head region in US imaging	Multi-scale mini-LinkNet network	N/A	12 and 40 weeks	DSC: 0.9265 Difference (DF): 0.94 mm Absolute Difference (ADF): 2.39 mm HD: 3.53 mm	1) methodology is clear. 2) result is blur for reader. 3) no cross validation is applied	
[86]	To locate the fetal head from 3D ultrasound images using shape model	AdaBoost	Shape Model Marginal Space Haar-like features	11 to 14 weeks	ACC: 0.7593	1) Methodology could be interpreted in better way. 2) Dataset very small. 3) Only accuracy as performance metrics.	
[84]	To detect fetal head	Deep Belief Network (DBN) Restricted Boltzmann Machines	Hough transform Histogram Equalization	11 to 14 weeks	ACC: 0.948 HD: 5.2033 Similarity Index (SI): 0.8472	1) Methodology is clear. 2) Only clinical dataset was reported and synthetic data were ignored. 3) Important performance metrics are missing.	
[88]	To semantically segment fetal head from maternal and other fetal tissue	U-NET	Ellipse fitting	12 and 20 weeks	ACC: 0.77 Average Error as DF: 14.96 mm	1) methodology is clear. 2) Dataset very small even public dataset is available. 3) Important performance metrics are missing such as DSC	
[103]	To automatically discover and localize anatomical landmarks. measure the HC, TV, and the TC	CNN	Saliency maps	13 to 26 weeks	CSP LV/Cereb HC TV alignment errors: 9.8 4.1 7.1	1) Methodology and results are confusing for the reader 2) Dataset acquisition and splitting are clear 3) Important performance metrics are missing	
[95]	To demonstrate the effectiveness of hybrid method to segment fetal head	DU-Net	Scattering Coefficients (SC)	13 to 26 weeks	DSC: 0.9733 HD: 1.58 mm	1) Methodology could be explained better for the reader. 2) Dataset splitting is not apparent, and no validation. 3) Proposed method did not achieve the best result.	
[96]	To segment fetal head using Network Binarization	Depthwise Separable Convolutional Neural Networks DSCNNs.	Network Binarization	12 and 40 weeks	DSC: 0.9689	1) Methodology orientation is not structured. 2) no validation. 3) Important performance metrics are missing.	
[97]	To segment the fetal skull boundary and fetal skull for fetal HC measurement	U-NET	Squeeze and Excitation (SE) blocks	12 and 40 weeks	DSC: 0.9731 ADF: 2.69 mm	1) Methodology orientation is clear. 2) Slightly improvement compared with original model. 3) Other performance metrics are missing	
[98]	To automatic segment and estimate of HC ellipse.	Multi-Task network based on Link-Net architecture (MTLN)	Ellipse Tuner	12 and 40 weeks	DSC: 0.9684 DF: 1.13 mm	ADF: 2.12 mm HD: 1.72 mm	1) Methodology and results are clear 2) Proposal method did not obtain the best result compared to the current work.
[99]	To capture more information with multiple-channel convolution from US images	Multiple-Channel and Atrous MA-Net	Encoder and Decoder Module	N/A	Dice: 0.973 Rec: 0.978 ASD: 4.152 mm	Pre: 0.968 mm HD: 10.924 mm RMSD: 4.161 mm	1) Methodology and results are clear and detailed. 2) dataset acquisition is clearly explained no validation is applied. 3) proposal method achieved the best result compared to other works except in precision.
[89]	To automatic segment fetal ultrasound image and HC biometry	Deeply Supervised Attention-Gated (DAG) V-Net	Attention-Gated Module	12 and 40 weeks	DSC :0.9793 ADF :1.77 mm	DF: 0.09 mm HD: 1.27 mm	1) Methodology and result are clear and detailed. 2) Dataset acquisition is clearly explained, no validation is applied 3) Proposal method achieved the best result compared to other state-of-the-art methods except in DSC. 4) Provided many comparisons with state-of-the-art methods
[90]	To compound a new US volume containing the whole brain anatomy	U-NET + Incidence Angle Maps (IAM)	CNN Normalized Mutual Information (NMI)	13 to 26 week	DSC: 0.811	AUC: 0.834	1) methodology and result are confusing for the reader. 2) dataset acquisition and splitting are not clearly defined. 3) paper organization is poor. 4) no comparison with state-of-the-art methods.
[161]	To directly measure the head circumference, without having to resort the handcrafted features or manually labeled segmented images.	CNN regressor (Reg-Resnet50)	N/A	12 to 40 weeks	MSE: 36.21 pixels MAE: 37.34 pixels Huber Loss (HL): 38.18 pixels	1) Methodology and result are simply explained and understandable. 2) Dataset acquisition and splitting are clearly defined. 3) Paper organization is poor. 4) First attempt to use CNN as a regressor to deal with fetal dataset without segmentation.	
[105]	To propose region-CNN for head localization and centering, and a regression CNN for accurately delineate the HC	CNN regressor (U-net)	Tiny-YOLOv2	12 to 40 weeks	DSC: 0.9776 ADF: 1.90 mm	DF: 0.21 mm HD: 1.32 mm	1) Methodology and result are simply explained and understandable. 2. Dataset acquisition and splitting are clearly defined. 3) Second attempt to use CNN as a regressor to deal with fetal HC dataset without segmentation
[102]	To present a novel end-to-end deep learning network to automatically measure the fetal HC, biparietal diameter (BPD), and occipitofrontal diameter (OFD) length from 2D US images	FCNN (SAPNet)	Regression network	12 to 40 weeks	DSC: 0.9772 ADF: 2.03 mm Mean Pixel ACC (mPA): 98.02	mIoU: 0.9646 HD: 0.47 mm	1) Methodology is clear, result has multiple comparisons confused the reader. 2) Dataset volume after augmentation were not reported. 3) regression network was not clarified
[104]	To segment fetal head from US images	FCN	Faster R-CNN	12 to 40 weeks	DSC: 0.9773 ADF: 2.33 mm	DF: 1.49 mm HD: 1.39 mm	1) Methodology is precise. 2) Dataset after augmentation is not reported. 3) No validation method, no comparison
[106]	To deals with a completely computerized detection device of next fetal head composition	Multi-Task network based on Link-Net architecture (MTLN)	Hadamard Transform (HT) ANN Feed Forward (NFFE) Classifier	N/A	ACC: 0.97		1) Methodology and result is not precise. 2) Dataset acquisition and splitting are missing 3) No validation method, no comparison. 4) Only accuracy is reported 5) paper is not organized
[85]	To measure HC automatically	Random Forest Classifier	Haar-like features Ellifit method	18 to 33 weeks	DSC: 0.9666 Pre: 0.9684 Spec: 0.9672	RMSD: 1.77 mm Rec: 0.9680	1) Methodology and result are precise. 2) Dataset is small with no augmentation and data acquisition is not detailed. 3) No validation method 4) Rely on prior knowledge of gestational age and scanning depth
[100]	To determine measurements of fetal HC and BPD	FNC	N/A	18 to 22 weeks	HC Inter-expert Model MAE 2.16 1.99 BPD MAE 0.59 0.61 DSC 0.98 0.98		1) Methodology and result are precise 2) Dataset is large with no augmentation, and data acquisition is detailed 3) Comparison between expert annotation and model prediction
[163]	To segment the whole fetal head in US volumes	Hybrid attention scheme (HAS)	3D U-NET + Encoder and Decoder architecture for dense labeling	20 to 31 weeks	DSC: 0.9605 0.9242 HD boundaries: 4.60 mm	Jaccard Index (JI):	1) Methodology and result are precise and detailed. 2) Dataset is small but augmented to obtain high volume. 3) Comparison is provided with another model. 4) Claimed to be the first investigation about whole fetal head segmentation in 3D US, but many works done before them, such as [101], [112]-[114].
[91]	To segment fetal head using a flexibly plug-and-play module called vector self-attention layer (VSAL)	CNN	Vector Self-Attention Layer (VSAL) Context Aggregation Loss (CAL)	12 and 40 weeks	DSC: 0.971 Pixel ACC (PA): 0.99	HD: 3.234	1) Methodology and result are precise and detailed. 2) Dataset is public; no augmentation is used. 3) Comparison is provided with another models. 4) Paper overwhelmed with unnecessary details
[101]	To provide automatic framework for skull segmentation in fetal 3D US	Two-Stage Cascade CNN (2S-CNN) U-NET	Incidence Angle Map Shadow Casting Map	20 to 36 weeks	DSC: 0.83 Symmetric Surface Distance (SSD): 0.98 mm	Jaccard index (JI): 0.70	1) Methodology and result are precise. 2) Dataset is very small; the volume of data was not reported after the augmentation. 3) No validation method. 4) Claimed to be the first investigation about whole fetal head segmentation in 3D US, but many works done before them, such as [112]-[114].
[92]	To segment 2D ultrasound images of fetal skulls based on a V-Net architecture	Fully Convolutional Neural Network Combination (VNet-c)	N/A	12 to 40 weeks	DSC: 0.979 Pre: 0.976	Jl: 0.959 ACC: 0.988	1) Methodology and result are precise. 2) The volume of data was not reported after the augmentation. 3) No validation method. 4) Comparative results were added. 5) Paper could be organized in better way
[93]	To segment the cranial pixels in an ultrasound image using a random forest classifier	Random Forest Classifier	Simple Linear Iterative Clustering (SLIC) Haar Features	25 to 34 weeks	Pre: 0.9901 Rec: 98.11	ACC: 0.9722	1) Methodology and result are not precise. 2) Dataset is very small with no augmentation, and data acquisition and splitting are not clear. 3) No comparison with other models 4) Paper is poorly written and inconsistent.
[94]	To automatically estimate fetal HC	U-Net	Monte-Carlo Dropout	18 to 22 weeks	DSC: 0.982 ADF: 1.81	HD: 1.29	1) Methodology and result are not precise. 2) Dataset acquisition and splitting is not clear. 3) No validation method.
Brain standard plane							
[107]	To automatically recognize six standard planes of fetal brains.	CNN+ Transfer learning DCNN	N/A	18 to 22 weeks 40 th week	ACC: 0.910 Rec: 0.901	Pre: 0.855 F1: 0.900	1) Clear methodology 2) Multi dataset are used with data augmentation
[114]	To help the clinician or sonographer obtaining these planes of interest by finding the fetal head alignment in 3D US	Random forest classifier	Shape model and template deformation algorithm Hough transform	19 to 24 weeks.	Maximal error distance: 5.8 5.1	TC TV	1) Methodology is not clear many objectives in one flow 2) Dataset very small 3) Only error rate as performance metrics

Table 6. Continued

Study	Objective	Backbone Methods/Framework	Optimization/ Extractor methods	Fetal age	Best Obtained Result	observations
[109]	To segment the fetal cerebellum from 2D US images.	U-NET +ResNet (ResU-NET-C)	N/A	18 to 20 weeks	DSC: 0.87 Pre: 0.90 HD: 28.15 mm Rec: 0.86	1) Methodology and results are presented clearly. 2) Dataset is small but acquisition, and splitting are clear. 3) Important performance metrics are used
[116]	To detect multiple planes simultaneously in challenging 3D US datasets	Multi-Agent Reinforcement Learning (MARL)	RNN Neural Architecture Search (NAS) Gradient-based Differentiable Architecture Sampler (GDAS)	19 to 31 weeks	Dihedral angles between two planes (ANG): 9.75 difference between their ED towards the volume origin (DIS): 1.19 Structural Similarity Index (SSIM):	1) Methodology and result detailed written 2) Second work that used of RL with the fetal dataset 3) Some details are not necessary to be included 4) Such as great work need future work 5) Some performance metrics are missing
[118]	To detect standard plane and quality assessment	Multi-task learning Framework Faster Regional CNN (MF R-CNN)	N/A	14 to 28 weeks	Detection (mAP): 0.9404 Pre: 0.9776 Spec: 0.9833 ACC: 0.9625	1) Methodology and result are precise and detailed. 2) Dataset is transparent in terms of acquisition and splitting. 3) Classification module should adopt only one architecture instead of seven. 4) Detection only evaluated using mean average precision, where many metrics were used for classification
[119]	To tackle the automated problem of fetal biometry measurement with a high degree of accuracy and reliability	U-Net, CNN	Bounding-box regression (object-detection)	N/A	HC ACC: 0.9143 DSC: 0.9539	1) Methodology and result are not precise 2) Dataset is very small but transparent in terms of acquisition and splitting 3) Only accuracy and DSC were used as performance evaluation
[117]	To determine the standard plane in US images	Faster R-CNN	Region Proposal Network (RPN)	14 to 28 weeks	LS CP T CSP TV AP 0.94 0.93 0.81 0.87 0.44	1) Methodology and result are precise. 2) Dataset acquisition is not detailed 3) No validation method. 4) Only Average Precision (AP) is reported
[112]	To address the problem of 3D fetal brain localization, structural segmentation, and alignment to a referential coordinate system	Multi-Task FCN	Slice-Wise Classification	18 to 34 weeks	Alignment Error Average of HD: 9.3 mm Brain Segmentation JI: 0.82 Classification Mean ACC: 0.964 Average center deviation: 2.0 mm Average scale deviation: 2.3	1) Methodology and result are precise and detailed 2) Dataset is small with no augmentation 3) No comparison is provided for such a great work 4) Performance evaluation metrics should be used, such as AUC, DSC, F1 score
[113]	To simultaneously localize multiple brain structures in 3D fetal US	View-based Projection Networks (VP-Nets)	U-Net CNN	20 to 29 weeks	Pre:0.9262 Rec: 0.9239 F1: 0.9239	1) Methodology and result are precise and detailed. 2) Dataset is small, but augmentation volume was not reported. 3) Comparison is provided with other models
[108]	To automatically identify six fetal brain standard planes (FBSPs) from the non-standard planes.	Differential-CNN	Modified feature map	16 to 34 weeks	ACC: 0.9311 Rec: 0.9239 AUC: 0.937	1) Methodology and result are precise. 2) After augmented the dataset splitting details is missing. 3) Comparative results were added 4) Paper was organized in a consistent way
[110]	To obtain the desired position of the gate and Middle Cerebral Artery (MCA)	MCANet	Dilated Residual Network (DRN) Dense Upsampling Convolution (DUC) block	28 to 40 weeks	DSC: 0.768 Jl: 0.633	1) Some of related work were written in the methodology. 2) After augmented the dataset splitting details is missing. 3) Comparative results were added 4) First MCA dataset that should be public but not yet
[111]	To segment four important fetal brain structures in 3D US	Random Decision Forests (RDF)	Generalized Haar-features	18 to 26 weeks	CP PVC CSP Cerebellum DSC: 0.79 0.82 0.74 0.63	1) Methodology and result are not precise. 2) Dataset is very small with no augmentation, and data acquisition and splitting is not clear 3) No comparison 4) Paper is poorly written and inconsistent.
[115]	To automatically localize fetal brain standard planes in 3D US	Dueling Deep Q Networks (DDQN)	RNN-based Active Termination (AT) (LSTM)	19 to 31 weeks	TC TT Dihedral (ANG): 9.61 9.11 ED to origin (Dis): 3.40 2.66 SSIM: 0.69 0.70	1) Methodology and result are precise. 2) Dataset is small, acquisition and splitting is clear. 3) No validation method. 4) First work that use RL to localize fetal head
Brain diseases						
[123]	To evaluate the feasibility of CNN-based DL algorithms predicting the fetal lateral ventricular width from prenatal US images.	ResNet50	Faster R-CNN Class Activation Mapping (CAM)	22 to 26 weeks.	MAE of the predicted lateral ventricular :1.01 mm ACC: 0.981	1) Methodology and result are confusing for the reader; no table or figure was seen to conclude the findings. 2) Dataset splitting is not well explained 3) Paper organization is poor. 4) No comparison with state-of-the-art methods
[120]	To recognize and separate the studied US data into two categories: healthy (HL) and hydrocephalus (HD) subjects.	CNN	N/A	20 to 22 weeks.	ACC: 0.9720 Spec: 0.9823	1) methodology and result are explained and understandable. 2) dataset is minimal and has no augmentation 3) First attempt to identify hydrocephalus.
[124]	To automatic measurement of fetal lateral ventricles (LVs) in 2D US images.	Mask R-CNN	Feature Pyramid Networks (FPN) Region Proposal Network (RPN)	N/A	ACC: 0.96 Rec:0.9491	1) Methodology is clear. 2) Fetal GA was not reported. 3) No validation no augmentation. 4) First study proposing an automatic measurement method for
[121]	To apply binary classification for central nervous system (CNS) malformations in standard fetal US brain images in axial planes.	CNN	Split-view Segmentation	18 to 32 weeks	ACC: 0.963 Rec: 0.969	1) Methodology and result is clear. 2) Dataset is very big and transparent in terms of acquisition and splitting, but from the same center and many scanners were used. 3) No validation
[122]	To develop computer-aided diagnosis algorithms for five common fetal brain abnormalities.	Deep convolutional neural networks (DCNNs) VGG-net	U-net Gradient-Weighted Class Activation Mapping (Grad-CAM)	18 to 32 weeks	Pre: 0.95 F1: 0.95	1) Methodology and result are clear. 2) Dataset is very big and transparent in terms of acquisition and splitting, but from the same center and many scanners were used 3) is not the first attempt to develop algorithms that determine whether fetal brain images of standard axial neurosonographic planes (SANPs) are normal or abnormal. 4) The localization of lesions was currently based purely on the CAM.

Table 7. Articles published using AI to improve fetus face monitoring: Objective, backbone methods, optimization, fetal age best result, and observations

Study	Objective	Backbone Methods/Framework	Optimization/ Extractor methods	Fetal age	Best Obtained Result	observations
Fetal facial standard plane (FFSP)						
[125]	To address the issue of recognition of standard planes (i.e., axial, coronal and sagittal planes) in the fetal ultrasound (US) image	SVM classifier	AdaBoost for detect region of interest, ROI) Dense Scale Invariant Feature Transform (DSIFT) Aggregating vectors for feature extraction fish vector (FV) Gaussian Mixture Model (GMM)	20 to 36 weeks	Mean Average Precision (mAP): 0.8995	1) Method and result are not clear. 2) Dataset is small, and the acquisition and splitting were not clear. 3) no data augmentation was not reported. 4) Other evaluation methods were not mentioned clearly
[126]	To automatically recognize the FFSP from US images	Deep convolutional networks (DCNN)	N/A	20 to 36 weeks	ACC: 0.9699 Rec: 0.9899	Pre:0.9698 1) Method and result are clear. 2) Dataset is small, and acquisition was not clear. 3) No data augmentation was not reported. 4) No validation method
[127]	To automatically recognize FFSP via a deep convolutional neural network (DCNN) architecture	DCNN	t-Distributed Stochastic Neighbor Embedding (t-SNE)	20 to 36 weeks	ACC: 0.9653 Rec: 0.97	Pre:0.9698 F1: 0.9699 1) Methodology and result is clear and detailed. 2) Dataset acquisition and splitting was clear. 3) Data augmentation and validation is employed 4) DCNN outperform
[128]	To automatic recognition of the fetal facial standard planes (FFSPs)	SVM classifier	Root scale invariant feature transform (RootSIFT) Gaussian mixture model (GMM) Fisher Vector (FV) Principle Component Analysis (PCA)	20 to 36 weeks	ACC: 0.9327	mAP: 0.9919 1) Multi-techniques were used in methodology and result is clear, detailed, and consistent. 2) Dataset acquisition and splitting was not clear. 3) Data augmentation and validation is not employed. 4) no comparison with other works. 5) For such great and detailed work, only precision and accuracy were reported.
[129]	To automatic recognize and classification of FFSPs	SVM classifier	Local Binary Pattern (LBP) Histogram of Oriented Gradient (HOG)	20 to 24 weeks	ACC: 0.9467 Rec: 0.9388	Pre:0.9427 F1:0.9408 1) Methodology and result are consistent. 2) Dataset splitting was not clear. 3) No data augmentation. 4) No comparison with other works.
Face anatomical landmarks						
[130]	To detect position and orientation of facial region and landmarks	SFFD-Net (Samsung Fetal Face Detection Network) multi-class segmented	N/A	14 to 30 weeks	L-Eye R-Eye Nose L2 norm (mm): 2.21 1.66 1.31	1) Method and result are not clear. 2) Dataset is small, and the acquisition and splitting was not clear. 3) Volume after data augmentation was not reported 4) Other evaluation methods were not mentioned
[131]	To detect landmarks in 3D fetal facial US volumes	CNN Backbone Network	Region Proposal Network (RPN) Bounding-box regression	N/A	AP: 0.8250	mIoU:0.6377 1) Method and result are clear. 2) Dataset is small, and acquisition was not clear. 3) Volume after data augmentation was not reported. 4) No validation method. 5) Other evaluation methods were not mentioned "
[132]	To detect nasal bone for US of fetus	Back Propagation Neural Network (BPNN)	Discrete Cosine Transform (DCT) Daubechies D4 Wavelet transform	11 to 13 weeks	Nasal Bone ACC:0.86 (43/50)	Without 0.88(44/50) 1) Methodology and result are inconsistent. 2. Dataset acquisition and splitting was not clear. 3) No data augmentation and validation are not employed 4) No comparison with other works.
Facial expressions						
[133]	To recognize facial expressions from 3D US	ANN	Histogram equalization Thresholding Morphing Sampling Clustering Local Binary Pattern (LBP) Minimum Redundancy and Maximum Relevance (MRMR)	N/A	ACC: 0.91 Rec: 0.85	Pre: 0.84 1) In methodology, multi-techniques were used. However, they can be replaced by using CNN. 2) Dataset is small, and the acquisition was not clear. 3) Data augmentation was not reported. 4) No validation method
[134]	To recognize fetal facial expressions that are considered as being related to the brain development of fetuses	CNN	N/A	19 to 38 weeks	ACC: 0.985 Rec: 0.996	Spec: 0.993 F1: 0.974 1) In methodology and result is clear. 2) Dataset acquisition was not clear. 3) volumes after data augmentation was not reported. 4) no validation method. 5) CNN outperform other method in [127] for a similar purpose.

Table 8. Articles published using AI to improve fetus heart monitoring: Objective, backbone methods, optimization, fetal age best result, and observations

Study	Objective	Backbone Methods/Framework	Optimization/ Extractor methods	Fetal age	Best Obtained Result	observations
Heart disease						
[137]	To perform multi-disease segmentation and multi-class semantic segmentation of the five key components	U-NET + DeepLabV3+	N/A	N/A	DSC:0.897 Cross Entropy Loss: 0.034	mIoU:0.720 1) Method and result are not clear. 2) dataset acquisition and splitting was not clear 3) no validation method 4) no comparison.
[139]	To recognize and judge Fetal congenital heart disease (FHD) development	DGACNN Framework	CNN Wasserstein GAN + Gradient Penalty (WGAN-GP) DANomaly Faster-RCNN	18–39 weeks	ACC: 0.850	AUC:0.881 1) Methodology and results are very detailed but confusing for the reader and could be written and organized consistent way. 2) Dataset is sufficient after the use of data augmentation. 3) Only ACC and AUC are reported. 4) Novel work and significant for clinical use.
[141]	To segment the ventricular septum in US	Cropping-Segmentation-Calibration (CSC)	YOLOv2 cropping module U-NET segmentation Module VGG-backbone Calibration Module	18 to 28 weeks	mDSC:0.6950	mIoU: 0.5598 1) Methodology and results are clear. 2) Many techniques were used to build the framework. 3) Dataset acquisition splitting is clear. 4) No data augmentation.
[140]	To detect cardiac substructures and structural abnormalities in fetal US videos	Supervised Object detection with Normal data Only (SONO)	CNN YOLOv2	18 to 34 weeks	Heart mean AUC: 0.787 cardiac substructure detection mAP: 0.702	Vessels 0.891 1) Two techniques were integrated to build the framework. 2) Methodology and result are clear. 3) Large dataset and no augmentation needed. 4) Supplement materials were added, including real-time record. 5) Significant work and first application were seen in this survey.
[138]	To identify recommended cardiac views and distinguish between normal hearts and complex CHD and calculate standard fetal cardiothoracic measurements	Ensemble of Neural Networks	ResNet and U-Net Grad-CAM	18 to 24 week	ACC: 0.90 Rec: 0.95 Negative predictive value in distinguishing normal from abnormal hearts: 100%	AUC:0.99 Spec: 0.96 1) Two modifies networks were used to build an ensemble framework 2) Methodology and results are very detailed, but a paper's organization is difficult for the reader. 3) Largest dataset in the field, acquisition, and splitting is clear 4) No comparison with other works. 5) Promising result was achieved.
[135]	To learn the features of Echogenic Intracardiac Focus (EIF) that can cause Down Syndrome (DS) whereas testing phase classifies the EIF into DS positive or DS negative based	Multi-scale Quantized Convolution Neural Network (MSQCNN)	Cross-Correlation Technique (CCT) Enhanced Learning Vector Quantiser (ELVQ)	24–26 weeks	ACC: 0.65 Spec: 0.50	Rec: 0.70 1) Methodology and result are not explained clearly. 2) Very small dataset, acquisition, and splitting was not clear. 3) No validation method, no data augmentation. 4) Evaluation metrics were not accurately reported.
[136]	To perform automated diagnosis of hypoplastic left heart syndrome (HLHS)	SonoNet (VGG16)	N/A	18–22 weeks	AUC: 0.93 Rec: 0.90	Pre: 0.83 F1: 0.87 1) Methodology is based on other work [164] result is explained clearly 2) Large dataset but data acquisition, and splitting was not clear 3) No validation method, no data augmentation. 4) No comparison with other works.

Table 8. Continued

Study	Objective	Backbone Methods/Framework	Optimization/ Extractor methods	Fetal age	Best Obtained Result	observations
Heart chamber's view						
[143]	To perform automated segmentation of cardiac structures	CU-NET	Structural Similarity Index Measure (SSIM)	N/A	DSC: 0.856 HD: 3.31 Pixel-level Accuracy (PA): 0.929	1) Methodology and results are clear. 2) No data augmentation and no validation method. 3) Dataset acquisition splitting is clear.
[144]	To accurately segment of seven important anatomical structures in the A4C view	DW-Net	Dilated Convolutional Chain (DCC) module W-Net module based on the concept of stacked U-Net	n/a	DSC: 0.827 AUC:0.990 PA:0.933	1) Methodology and results are clear. 2) Two techniques were used to build the framework. 3) Dataset splitting is not clear. 4) No data augmentation 5) Claimed to be first time that a CNN based deep learning method is applied in the segmentation of multiple anatomical structures in A4C views.
[146]	To automatic quality control of fetal US cardiac four-chamber plane	Three CNN-based Framework	Basic-CNN, a variant of SqueezeNet Deep-CNN with DenseNet-161 as basic architecture The ARVNet for real-time object detection.	14 to 28 weeks	ACC Pre Rec F1 B-CNN: 0.9983 0.9982 0.9983 0.9983 D-CNN: 0.9951 0.9849 0.9877 0.9863 mAP of ARVNet: 0.9352	1) Three different networks were used to build the framework. 2) Dataset splitting is not clear. 3) Each network was tested separately, and the average performance for the whole framework was not reported.
[147]	To localize the end-systolic (ES) and end-diastolic (ED) from ultrasound	Hybrid CNN based framework	YOLOv3 Maximum Difference Fusion (MDF) Transferred CNN	18 to 36 weeks	Pre Rec Spec F1 ES: 0.9569 0.9513 0.9427 0.9541 ED: 0.9490 0.9273 0.9547 0.9380 Average ACC: 0.9484	1) Many different techniques were integrated to build the framework. 2) Volume of the dataset after augmentation was not reported. 3) No validation method. 4) significant work and first-time MobileNet network were used to deal with the fetal US and achieved promising results.
[145]	To detect the fetal heart and classifying each individual frame as belonging to one of the standard viewing planes	FCN	N/A	20 to 35 weeks	Segmentation error rate: 0.2348	1) Methodology and result are clear. 2) Large dataset and volume after augmentation is not reported. 3) Only error rate is reported and no validation method.
[142]	To jointly predict the visibility, view plane, location of the fetal heart in US videos.	Multi-Task CNN	Hierarchical Temporal Encoding (HTE)	20 to 35 weeks	ACC: Classification 0.8358 Localization 0.7968	1) Methodology is not clearly explained. 2) dataset acquisition and splitting were not clear. 3) Only accuracy rate is reported, and no validation method

Table 9. Articles published using AI to improve fetus abdomen monitoring: method details, objectives, health issue, dataset details and model observations

Study	Objective	Backbone Methods/Framework	Optimization/ Extractor methods	Fetal age	Best Obtained Result	observations
Abdominal anatomical landmarks						
[148]	To automatically detect two anatomical landmarks in an abdominal image plane stomach bubble (SB) and the umbilical vein (UV).	AdaBoost	Haar-like feature	14 to 19 weeks	SB UV ACC: 0.80 0.63 Spec: 0.70 0.65 Rec: 0.86 0.73 Error: 0.19 0.36	1) Methodology is explained clearly but result need more details. 2) Dataset acquisition and splitting was clear. 3) No validation method, no data augmentation. 4) No comparison with other works.
[149]	To localize fetal abdominal standard plane (FASP) from US including SB, UV, and spine (SP)	Random Forests Classifier+ SVM	Haar-like feature Radial Component-Based Model (RCM)	18 to 40 weeks	Overall ACC: 0.816	1) Methodology and result are not clearly explained. 2) Dataset acquisition and splitting was not clear. 3) No validation method, no data augmentation. 4) Only detection rate was used to evaluate the performance.
[155]	To classify ultrasound images (SB, amniotic fluid (AF), and UV) and to obtain an initial estimate of the AC."	Initial Estimation CNN+U-Net	Hough transform	N/A	DSC AC measurement: 0.9255 Abdominal Plane acceptance ACC: 0.871	1) Many networks were used to build none integrated framework; methodology and results are confusing for the reader. 2) Dataset acquisition and splitting was not clear. 3) No validation method. 4) Evaluation metrics were not used clearly. 5)
[157]	To classify ultrasound images (SB, AF, and UV) and measure AC	CNN	Hough transform	20 to 34 weeks	DSC AC measurement: 0.8919 Abdominal Plane acceptance ACC: 0.809	1) Many networks were used to build none integrated framework; methodology and results are confusing for the reader. 2) Dataset acquisition and splitting was not clear. 3) No validation method 4) Evaluation metrics were not used clearly. 5)
[150]	To find the region of interest (ROI) of the fetal abdominal region in the US image.	Fetal US Image Quality Assessment (FUIQA)	L-CNN is able to localize the fetal abdominal ROI AlexNet C-CNN then further analyzes the identified ROI DCNN to duplicate the US images for the RGB channels	16 to 40 weeks	SB UV AUC: 0.999 0.996 ACC: 0.990 0.983	1) Many networks were used to build the FUIQA framework. 2) Methodology and results are confusing for the reader. 3) Dataset splitting was not clear 4) No validation method 5) No comparison
[151]	To localize the fetal abdominal standard plane from ultrasound	Random forest classifier+ SVM classifier	Radial Component-based Model (RCM) Vessel Probability Map (VPM) Haar-like features	18 to 40 weeks	SB UV SP ROI AUC: 0.99 0.99 0.99 0.98 Overall ACC: 0.856	1) Two classifiers were used to improve detection speed and accuracy. 2) Methodology is not consistently explained. 3) Dataset splitting was not clear after data Augmentation. 4) No validation method
[156]	To diagnose the (prenatal) US-images by design and implement a novel framework	Defending Against Child Death (DACD)	CNN U-Net Hough-man transformation	N/A	SB UV class ACC: 0.991 0.996 0.996 Overall ACC: 99.7	1) Classification integrated with segmentation was used to improve detection speed and accuracy. 2) Methodology is not consistently explained. 3) Dataset splitting was not precise, no augmentation. 4) No validation method. 5) Some inconsistency during the comparison with other works, however, DACD provide promising results.
[152]	To detect important landmarks employed in manual scoring of ultrasound images.	AdaBoost	Haar-like feature	18 to 37 weeks	SB UV ACC: 0.7894 0.6280 AUC: 0.80 0.57	1) Methodology and result is clear but not detailed 2) Dataset acquisition and splitting are missing; no augmentation. 3) No validation method. 4) No comparison with other works.
[154]	To automatically select the standard plane from the fetal US volume for the application of fetal biometry measurement.	AdaBoost	One Combined Trained Classifier (1CTC) Two Separately Trained Classifiers (2STC) Haar-like feature	20 to 28 weeks	Rec: 0.9129 Pre: 0.7629	1) Methodology is clear but result missing more detailed 2) Dataset acquisition and splitting is missing. 3) No validation method. 4) No comparison with other work. 5) First work in the area.
[153]	To localize the FASP from US images.	DCNN	Fine Tuning with Knowledge Transfer Barnes-Hut Stochastic Neighbor Embedding (BH-SNE)	18 to 40 weeks)	ACC: 0.910	1) Methodology is not clear. 2) Dataset acquisition and splitting are precise, and data augmentation was reported. 3) No validation method. 4) Comparison with other works 5) Only accuracy was reported.

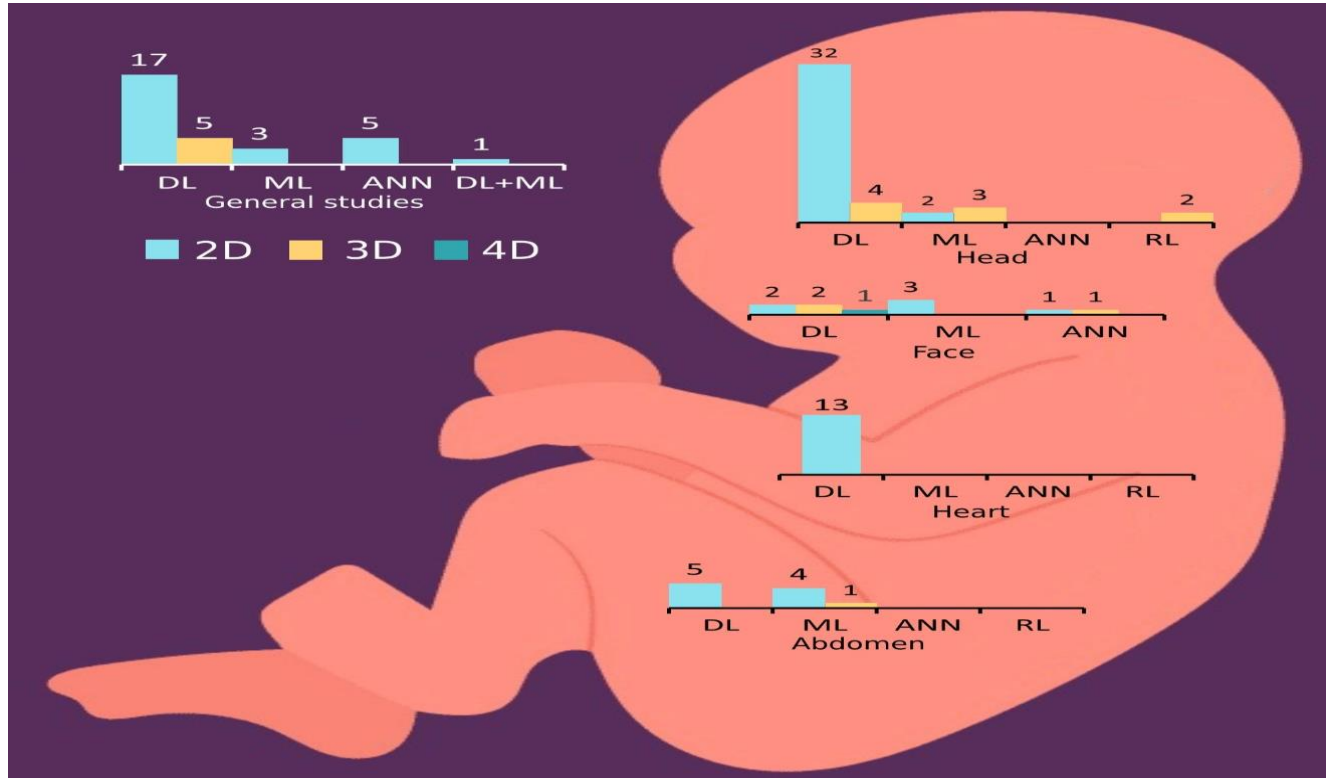


Figure 4. AI techniques that used within all studies in this survey. AI techniques are ordered by US images type and further categorized by fetal organ. Totals here equal the number of included papers.

6. Discussion

6.1 Principal findings

AI techniques applied are shown in [Figure 4](#). Deep learning (DL) was the most utilized techniques, seen in ($n=81$, 75.70%) studies. Traditional Machine learning (ML) models are used in ($n=16$, 14.95%) studies. Artificial neural network (ANN) models are only used in ($n=7$, 6.5%) studies. We also found the use of Reinforcement learning (RL) in ($n=2$, 1.86%) studies. Both deep learning as well as machine learning models were used in one study.

- **Deep learning for fetus health**

As seen in [Figure 4](#). DL was used heavily in all fetal organ experiments including general fetus issues, fetus head, fetus face, fetus heart, and fetus abdomen. Furthermore, as seen in most of the models ($n=74$, 69.1%), Convolutional Neural Network (CNN) used as a backbone of deep learning and is used in all tasks including classification, segmentation and object detection [54], [56], [57], [59], [63], [65]–[68], [72], [73], [76], [77], [81], [82], [84], [87]–[91], [93]–[99], [102]–[107], [109], [110], [113], [117]–[124], [126], [127], [130], [131], [134]–[144], [146], [147], [150], [153], [155]–[157], [161], [163]. Additionally, Fully Connected Neural Networks (FCNNs) is similarly largely utilized as a backbone or part of the framework ($n=11$, 10.28%) of DL, as seen in [63], [65], [70], [71], [80], [92], [100], [104], [112], [145], [146]. In addition to CNN and FCN, a Recurrent Neural Network (RNN) used to perform classification tasks in hybrid frameworks as seen in ($n=5$, 4.67%) studies [54], [57], [59], [60], [70]. U-Net is a convolutional neural network that was developed for biomedical image segmentation. Therefore, we found U-NET to be the most frequently utilized segmentation model as a baseline of the framework or as optimization. This was seen in ($n=23$, 21.50%) [63], [73], [81], [82], [88], [90], [94], [95], [97], [101], [109], [113], [118], [119], [122], [137], [138], [141], [143], [144], [155], [156], [163]. Other segmentation models were also used, such as DeepLabV3 in [137], LinkNet in [106], and the Encoder-Decoder network based on VGG16 in [72]. A Residual Neural Network (ResNet) was used to perform some tasks and enhance the framework efficiency as seen in ($n=6$, 5.60%) studies [62], [67], [82], [109], [110], [123], [138]. Some popular object detection models ($n=12$, 11.21%) were utilized to perform detection tasks in the fetus head, face, and heart. Additionally, Region Proposal Network

(RPN) with bounding-box regression technique was used in [119], [131]. Faster R-CNN was utilized in [104], [117]–[119]. Further, YOLO (You Only Look Once) models were utilized; YOLOv2 in [105], [140], [141] and YOLOv3 in [147]. Mask R-CNN was utilized only in [124] and Aggregated Residual Visual Block (ARVB) was used only in [146]. Surprisingly, we have found CNN is used for regression to predict the accurate measurement of HC as seen in [102], [103], [105], [161]. We found that, due to the noise and characteristics of US images, DL still relies on traditional feature extraction techniques in image analysis used to optimize the DL frameworks for better performance. For example, Hough transform was utilized with head and abdomen US images as seen in [84], [155]–[157]. Additionally, image processing techniques such as histogram equalization was used in [84]. Besides these tools, Class Activation Maps (CAM) are a helpful classification tool in computer vision that was utilized for brain visualization in [122], [123], fetal part structure in [54], and heart chamber view in [138]. DL shows promising results for the identification of certain fetus diseases as seen in the identification of heart diseases [135]–[141], brain diseases [120]–[124], and growth diseases [75]–[77]. Table 10 list of DL studies exhibiting technical novelty that achieved promising results in each category.

Table 10. Best DL study in each category based on the achieved result

Mian Organ	Sub-section	Best study
Fetal Body	Fetal part structures	[62], [65]
	Anatomical structures	[67], [73]
	Growth disease	[77]
	Gestational age	[81]
Head	Skull localization	[105], [161]
	Brain Standard plan	[107], [108], [110]
	Brain disease	[120], [124]
Face	Fetal facial standard	[127]
	Face anatomical	[130]
	Facial expression	[134]
Heart	Heart disease	[135], [137], [138], [140]
	Heart chamber view	[144], [147]
Abdomen	Abdominal anatomical	[155], [156]

- **Machine learning for fetus health**

Most of the research utilizing machine learning for fetal health monitoring was conducted between 2010 and 2015, as seen in (n=14, 13.8%). Only two studies [85], [129] were published in 2018 and 2021, respectively. We found that ML models were used for all fetus organs except for the heart and identification of fetus disease. The most used ML algorithm was Random Forest (RF), as seen in (n=8, 7.47%) studies. RF was used as a baseline classifier in [85], [93], [111], [114]. RF was used with other classifiers as well, with Support Vector Machine (SVM) in [149], [151] and Probabilistic Boosting Tree (PBT) in [55]. Simple Linear Iterative Clustering (SLIC) was also used in [64]. The SVM classifier was used in (n=6, 5.60%) studies. SVM was used as a baseline classifier in [53], [125], [128], [129] and utilized with other classifiers as seen in [149], [151]. AdaBoost was used in (n=5, 4.67%) studies as a baseline classifier in [86], [148], [152], [154] and to detect the region of interest (ROI) in [125]. Moreover, ML traditional algorithm still rely on Haar-like features (digital image features used in object recognition) while being utilized with US images as seen in (n=9, 8.41%) studies [85], [86], [93], [111], [148], [149], [151], [152], [154]. Gaussian Mixture Model (GMM) and Fisher Vector (FV) were used in (n=3, 2.80%) studies, where GMM is used to simulate the distribution of extracted characteristics throughout the images. Then, FV represents the gradients of the features under the GMM, with respect to the GMM parameters as seen in [53], [118], [125].

DL and ML models were seen in [58]. the SVM with decision fusion for classification and features extracted by fine-tuning AlexNet. Finally, we found the first research to utilize ML model in monitoring fetus health was in [154], which used to classify abdominal anatomical landmarks.

- **Artificial Neural Network for fetus health**

ANN is the cut edge between ML and DL [165]. As seen in Figure 4, ANN was used in (n=7, 6.5%) studies [69], [74], [78], [79], [83], [132], [133]. ANN models were used for the identification of growth diseases [74], [78], [79], fetus gender [83], facial expressions [133], face anatomical landmarks (Nasal Bone) [132], and anatomical structures (nuchal translucency (NT)) [69]. Hence, ANN was not utilized to identify brain or heart structures, nor accompanying disease. Finally, we concluded that the first utilization of ANN to monitor fetus health was in 2010 [69]; the main goal was to detect NT, which helps early identify Down syndrome. The second utilization of ANN was completed in 2011 [132] to detect nasal bone. This detection also helps for early identification of Down syndrome.

- **Reinforcement learning for fetus health**

The first attempt to utilize RL to monitor fetus health was in 2019 [115]. Dueling Deep Q Networks (DDQN) was employed with RNN-based active termination (AT) to identify brain standard planes (trans-thalamic (TT) and trans-cerebellar (TC)). The second time RL was utilized to monitor fetus health was reported on in a recent study from 2021 [116]. A multi-agent RL (MARL) was used in a framework that comprises RNN and includes both neural architecture search (NAS) as well as gradient-based differentiable architecture sampler (GDAS). This framework achieved promising results for identifying the brain standard plane and localize mid-sagittal, transverse (T), coronal (C) planes in volumes, trans-thalamic (TT), trans-ventricular (TV), and trans-cerebellar (TC).

6.1.1 Strengths

To the best of our knowledge, this survey is the first to explore all AI techniques implemented to provide fetus health care and monitoring during different pregnancy trimesters. This survey may be considered comprehensive as it does not focus on specific AI branches or diseases. Rather, it provides a holistic view of AI's role in monitoring fetuses via ultrasound images. This survey will benefit both readers, first medical professionals to have sight about the current AI technology in a development stage and assist data scientists in overcoming existing research and implication problems. secondly, for data scientists to continue future investigating in developing lightweight models and overcoming problems that slow the transformation of this technology based on a solid guideline proposed by the medical professionals. It may be considered a robust and high-quality survey. Because the most prominent health and information technology databases were searched using a well-developed search query, the search was sensitive and exact. Lastly, the utilization of techniques like scanning

grey literature databases (Google Scholar), biomedical literature database (PubMed, Embase) World's leading citation databases (Web of Science), Subject Specific Databases (PsycINFO), and world's leading source for scientific, technical, and medical research (ScienceDirect, IEEE explore, ACM Library) indicates that this study's risk of publication bias is low.

6.1.2 Limitations

A comprehensive systematic survey was conducted. However, the search within the databases was conducted between 22nd and 23rd June 202, so we might miss some new studies. Besides that, the words "pregnancy" or "pregnant" or "uterus" were not used as search terms to identify relevant papers. Therefore, some fetus health monitoring studies might have been missed, lowering the overall number of studies. Additionally, this survey focused more on a clinical rather than the technical; therefore, some technical details may have been missed. Lastly, only English studies were included in the search. As a result, research written in other languages was excluded.

6.2 Practical and research implication

The diagnosis of US imaging plays a significant role in clinical patient care. Deep learning, especially the CNN-based model, has lately gained much interest because of its excellent image recognition performance. If CNN were to live up to its potential in radiology, it is expected to aid sonographers and radiologists in achieving diagnostic perfection and improving patient care [166]. Diagnostic software based on artificial intelligence is vital in academia and research and has significant media relevance. These systems are largely based on analyzing diagnostic images, such as X-RAY, CT, MRI, electrocardiograms, and electroencephalograms. In contrast, US imaging, which is non-invasive, non-expensive, and non-ionizing, has limited AI applications compared to other radiology imaging technologies [167].

This survey found one available AI-based application to identify fetal cardiac substructures and indicate structural abnormalities as seen in [140]. From these findings, many studies achieved promising results in diagnosing fetus diseases or identifying specific fetus landmarks. However, to the best of our knowledge there is no randomized controlled trial (RCT) or pilot study carried out at a medical center or any adaptation of an AI-based application at any hospitals. This hesitance could be due to the following challenges [167]; 1) The present AI system can complete tasks that radiologists are capable of but may make mistakes that a radiologist would not make. For example, radiologists may not see undetectable modifications to the input data. These changes may not be seen by human eyes but would nevertheless impact the result of AI system's categorization. In other words, a tiny variation might cause a deep learning system to reach a different result or judgment. 2) Developers require a specific quantity of reliable and standardized data with an authorized reference standard to train AI systems. Annotated images may become an issue if this is done through retroactive research. Datasets may also be difficult to get as the firms that control them want to keep them private and preserve their intellectual property. Validation of an AI system in the clinic can be difficult as it frequently necessitates multi-institutional collaboration and efficient communication between AI engineers and radiologists. Validating an AI system is also expensive and time-consuming. Finally, 3) when extensive patient databases are involved, ethical and legal concerns may arise.

This survey found some of these challenges were addressed in some studies. For example, applying transfer learning on AI model learned natively on US images and fine-tuning the model on an innovative data set collected from a different medical center and/or different US equipment. Another way to address the challenges of a small data set is to employ data augmentation (e.g., tissue deformation, translations, horizontal flips, adding noise, and images enhancement) to boost the generalization capacity of DL models. It is recommended that data augmentation settings should be carefully chosen to replicate ultrasound images' changes properly [168]. Advanced AI applications are already being used in breast and chest imaging. Large quantities of medical images with strong reference standards are accessible in various fields, allowing the AI system to be trained. Other subspecialties like fetus disease, musculoskeletal disease or interventional radiology are less familiar with utilizing AI. However, it seems that in the future, AI may influence every medical application that utilizes any images [169].

This survey found that no standard guideline is being followed or developed that focused on AI in diagnostic imaging to meet clinical setting, evaluation, and requirements. Therefore, the Radiology Editorial Board [170] has created a list of nine important factors to assist in evaluating AI research as a first step. These recommendations are intended to enhance the validity and usefulness of AI research in diagnostic imaging. These issues are outlined for authors, although manuscript reviewers and readers may find them useful as well: 1) Carefully specify the AI experiment's three image sets (training, validation, and test sets of images). 2) For final statistical reporting, use a separate test set. Overfitting is a problem with AI models, which means they only function for the images they are trained to recognize. It is ideal to utilize an outside collection of images (e.g., the external test set) from another center. 3) Use multivendor images for each step of the AI assessment, if possible (training, validation, test sets). Radiologists understand medical images from one vendor are not identical to theirs; radiomics and AI systems can help in identifying changes in the images. Moreover, multivendor AI algorithms are considerably more interesting than vendor-specific AI algorithms. 4) Always justify the training, validation, and test sets' sizes. Depending on the application, the number of images needed to train an AI system varies. After just a few hundred images, an AI model may be able to learn image segmentation. 5) Train the AI algorithm using a generally recognized industry standard of reference. For instance, chest radiographs are interpreted by a team of experienced radiologists. 6) Describe any image processing for the AI algorithm. Did the authors manually pick important images, or crop images to a limited field of view? How images are prepared and annotated has a big impact on radiologist's comprehension of the AI model. 7) Compare AI performance against that of radiology professionals. Competitions and leader boards for the "best" AI are popular among computer scientists working in the AI field. The area under the receiver operating characteristic curve is often used to compare one AI to another (AUC). On the other hand, physicians are considerably more interested in comparing the AI system to expert readers, when treating a patient. Experienced radiologist readers are recommended to benchmark an algorithm intended to identify radiologic anomalies. 8) Demonstrate the AI algorithm's decision-making process. As previously mentioned, computer scientists working on imaging studies often describe their findings as a single AUC/ACC number. This AUC/ACC is compared to the previous best algorithm, which is a competitor. Unfortunately, the AUC/ACC value has little bearing on clinical medicine on its own. Even with a high AUC/ACC of 0.95, there may be an operating mode in which 99 out of 100 anomalies are overlooked. Many research teams overlay colored probability maps from the AI on the source images to assist doctors in comprehending the AI performance. 9) The AI algorithm should be open source so performance claims may be independently validated; this is already a prevalent recommendation, as this survey found only (n=9, 8.4%) studies [62], [70], [92], [105], [138]–[141], [163] made their works publicly available.

7. Future work and conclusion

Throughout this survey, various ways that AI techniques have been used to improve fetal care during pregnancy have been discussed, including: 1) determining the existence of a live embryo/fetal and estimate the pregnancy's age, 2) identifying congenital fetus defects and determining the fetus's location, 3) determining the placenta's location, 4) checking for cervix opening or shortening and evaluating fetal development by measuring the quantity of amniotic fluid surrounding the baby, 5) evaluating the fetus's health and see whether it is growing properly. Unfortunately, due to both ethical and privacy concerns as well as the reliability of AI decisions, all aspects of these models are not yet utilized as end applications in medical centers.

Undergraduate sonologist education is becoming more essential in medical student careers; consequently, new training techniques are necessary. As seen in other medical fields, AI-based applications and tools were employed for medical and health informatics students [171]. Moreover, AI-mobile-based applications were useful for medical students,

clinicians, and allied health workers alike [172]. To the best of our knowledge, there are no AI-based mobile applications available to assist radiologist or sonographer students in medical college. Besides that, medical students may face many challenges during fetal US scanning [173]. Therefore, our future work will propose an AI- mobile-based application to help radiology or sonography students identify features in fetus US image and answer the following research questions: 1) How is the lightweight model efficient and accurate when localizing the fetal head, abdomen, femur, and thorax from the first to the third trimester?; 2) How efficient and accurate the lightweight model will identify the fetal gestational age (GA) from the first to the third trimester?; 3) How will inter-rater reliability tests validate the proposed model and compare the obtained result with experts and students using the intra-class correlation coefficient (ICC) [174]?

We have concluded that AI techniques utilized US images to monitor fetal health from different aspects through various GA. Out of 107 studies, DL was the most widely used model, followed by ML, ANN, and RL. These models were used to implement various tasks, including classification, segmentation, object detection, and regression. We found that even the most recent studies rely on the 2D US followed by 3D, and that 4D is rarely used. Furthermore, we found that most of the work was targeted the fetus head followed by the body, heart, face, and abdomen. We identified the lead institutes in this field and their research.

This survey discusses the availability of the dataset for each category and highlighted their promising result. In addition, we analyzed each study independently and provided observations for the future reader. All optimization and feature extraction methods were reported for each study to highlight the unique contribution. Moreover, DL novel and unique works were highlighted for each category. The research and practical implications were discussed, and prospective research and clinical practitioner recommendations were provided. Finally, a future research direction has been proposed to answer the gap in this survey.

Key Points

- Artificial intelligence and machine learning methods can be successfully employed to optimize fetus care.
- Deep learning methods are the most common approach to monitor fetal health ,and the fetal head analysis is gaining traction.
- Future research should focus on employing these technologies and developing an actual application that can be used at medical colleges and centers.

Supplementary data

Multimedia Appendix 1: Search strings

Multimedia Appendix 2: Data extraction form

Data Availability Statement

Available upon request

Funding

No funding

Conflicts of Interest

None declared

References

- [1] D. Hassabis, D. Kumaran, C. Summerfield, and M. Botvinick, "Neuroscience-Inspired Artificial Intelligence," *Neuron*, vol. 95, no. 2, pp. 245–258, Jul. 2017, doi: 10.1016/j.neuron.2017.06.011.
- [2] D. D. Miller and E. W. Brown, "Artificial Intelligence in Medical Practice: The Question to the Answer?," *Am. J. Med.*, vol. 131, no. 2, pp. 129–133, Feb. 2018, doi: 10.1016/j.amjmed.2017.10.035.
- [3] P. Savadjiev *et al.*, "Demystification of AI-driven medical image interpretation: past, present and future," *European Radiology*, vol.

- 29, no. 3. Springer Verlag, pp. 1616–1624, Mar. 02, 2019. doi: 10.1007/s00330-018-5674-x.
- [4] N. Shahid, T. Rappon, and W. Berta, “Applications of artificial neural networks in health care organizational decision-making: A scoping review,” *PLoS ONE*, vol. 14, no. 2. Public Library of Science, Feb. 01, 2019. doi: 10.1371/journal.pone.0212356.
- [5] M. Fatima and M. Pasha, “Survey of Machine Learning Algorithms for Disease Diagnostic,” *J. Intell. Learn. Syst. Appl.*, vol. 09, no. 01, pp. 1–16, 2017. doi: 10.4236/jilsa.2017.91001.
- [6] M. Kim et al., “Deep learning in medical imaging,” *Neurospine*, vol. 16, no. 4, pp. 657–668, Dec. 2019. doi: 10.14245/ns.1938396.198.
- [7] I. Castiglioni et al., “AI applications to medical images: From machine learning to deep learning,” *Phys. Medica*, vol. 83, pp. 9–24, Mar. 2021. doi: 10.1016/j.ejpm.2021.02.006.
- [8] H. Fujita, “AI-based computer-aided diagnosis (AI-CAD): the latest review to read first,” *Radiol. Phys. Technol.*, vol. 13, no. 1, pp. 6–19, Mar. 2020. doi: 10.1007/s12194-019-00552-4.
- [9] X. Tang, “The role of artificial intelligence in medical imaging research,” *BJR/Open*, vol. 2, no. 1, p. 20190031, Nov. 2020. doi: 10.1259/bjro.20190031.
- [10] R. C. Deo, “Machine learning in medicine,” *Circulation*, vol. 132, no. 20, pp. 1920–1930, Nov. 2015. doi: 10.1161/CIRCULATIONAHA.115.001593.
- [11] G. S. Handelman, H. K. Kok, R. V. Chandra, A. H. Razavi, M. J. Lee, and H. Asadi, “eDoctor: machine learning and the future of medicine,” *J. Intern. Med.*, vol. 284, no. 6, pp. 603–619, Dec. 2018. doi: 10.1111/joim.12822.
- [12] R. Miotto, F. Wang, S. Wang, X. Jiang, and J. T. Dudley, “Deep learning for healthcare: Review, opportunities and challenges,” *Brief. Bioinform.*, vol. 19, no. 6, pp. 1236–1246, 2017. doi: 10.1093/bib/bbx044.
- [13] G. A. Cheikh, A. B. Mbacke, and S. Ndiaye, “Deep learning in medical imaging survey,” *CEUR Workshop Proc.*, vol. 2647, pp. 111–127, 2020. Accessed: Aug. 13, 2021. [Online]. Available: <https://www.ncbi.nlm.nih.gov/pmc/articles/PMC6945006/>
- [14] B. Raef and R. Ferdousi, “A review of machine learning approaches in assisted reproductive technologies,” *Acta Inform. Medica*, vol. 27, no. 3, pp. 205–211, 2019. doi: 10.5455/aim.2019.27.205-211.
- [15] J. Balayla and G. Shrem, “Use of artificial intelligence (AI) in the interpretation of intrapartum fetal heart rate (FHR) tracings: a systematic review and meta-analysis,” *Arch. Gynecol. Obstet.*, vol. 300, no. 1, pp. 7–14, Jul. 2019. doi: 10.1007/s00404-019-05151-7.
- [16] P. M. Iftikhar, M. V. Kuijpers, A. Khayyat, A. Iftikhar, and M. DeGouviva De Sa, “Artificial Intelligence: A New Paradigm in Obstetrics and Gynecology Research and Clinical Practice,” *Cureus*, 2020. doi: 10.7759/cureus.7124.
- [17] Z. Chen, Z. Liu, M. Du, and Z. Wang, “Artificial Intelligence in Obstetric Ultrasound: An Update and Future Applications,” *Front. Med.*, vol. 8, p. 1431, Aug. 2021. doi: 10.3389/fmed.2021.733468.
- [18] C. Sen, “Preterm labor and preterm birth,” *J. Perinat. Med.*, vol. 45, no. 8, pp. 911–913, Nov. 2017. doi: 10.1515/jpm-2017-0298.
- [19] P. J. Correa, Y. Palmeiro, M. J. Soto, C. Ugarte, and S. E. Illanes, “Etiopathogenesis, prediction, and prevention of preeclampsia,” *Hypertens. Pregnancy*, vol. 35, no. 3, pp. 280–294, Jul. 2016. doi: 10.1080/10641955.2016.1181180.
- [20] E. C. Larsen, O. B. Christiansen, A. M. Kolte, and N. Macklon, “New insights into mechanisms behind miscarriage,” *BMC Med.*, vol. 11, no. 1, Jun. 2013. doi: 10.1186/1741-7015-11-154.
- [21] Z. Chen, Z. Wang, M. Du, and Z. Liu, “Artificial Intelligence in the Assessment of Female Reproductive Function Using Ultrasound: A Review,” *J. Ultrasound Med.*, 2021. doi: 10.1002/jum.15827.
- [22] D. Avola, L. Cinque, A. Fagioli, G. Foresti, and A. Mecca, “Ultrasound Medical Imaging Techniques,” *ACM Computing Surveys*, vol. 54, no. 3. 2021. doi: 10.1145/3447243.
- [23] M. Whitworth, L. Bricker, and C. Mullan, “Ultrasound for fetal assessment in early pregnancy,” *Cochrane Database Syst. Rev.*, vol. 2015, no. 7, Jul. 2015. doi: 10.1002/14651858.CD007058.pub3.
- [24] P. Garcia-Canadilla, S. Sanchez-Martinez, F. Crispi, and B. Bijlens, “Machine Learning in Fetal Cardiology: What to Expect,” *Fetal Diagn. Ther.*, vol. 47, no. 5, pp. 363–372, 2020. doi: 10.1159/000505021.
- [25] S. P. Arjunan and M. C. Thomas, “A Review of Ultrasound Imaging Techniques for the Detection of Down Syndrome,” *Irbm*, vol. 41, no. 2. pp. 115–123, 2020. doi: 10.1016/j.irbm.2019.10.004.
- [26] J. Hartkopf, J. Moser, F. Schlegler, H. Preissl, and J. Keune, “Changes in event-related brain responses and habituation during child development – A systematic literature review,” *Clin. Neurophysiol.*, vol. 130, no. 12, pp. 2238–2254, 2019. doi: 10.1016/j.clinph.2019.08.029.
- [27] O. J. Shiney, J. A. P. Singh, and B. P. Shan, “A Review on techniques for computer aided diagnosis of soft markers for detection of down syndrome in ultrasound fetal images,” *Biomed. Pharmacol. J.*, vol. 10, no. 3, pp. 1559–1568, 2017. doi: 10.13005/bpj/1266.
- [28] J. Torrents-Barrena et al., “Segmentation and classification in MRI and US fetal imaging: Recent trends and future prospects,” *Med. Image Anal.*, vol. 51, pp. 61–88, 2019. doi: 10.1016/j.media.2018.10.003.
- [29] P. Kaur, G. Singh, and P. Kaur, “A Review of Denoising Medical Images Using Machine Learning Approaches,” *Curr. Med. Imaging Rev.*, vol. 14, no. 5, pp. 675–685, 2017. doi: 10.2174/1573405613666170428154156.
- [30] L. Davidson and M. R. Boland, “Towards deep phenotyping pregnancy: a systematic review on artificial intelligence and machine learning methods to improve pregnancy outcomes,” *Brief. Bioinform.*, 2021. doi: 10.1093/bib/bbaa369.
- [31] S. Al-yousif et al., “A systematic review of automated preprocessing, feature extraction and classification of cardiocography,” *PeerJ Comput. Sci.*, vol. 7, pp. 1–37, 2021. doi: 10.7717/peerj-cs.452.
- [32] M. Komatsu et al., “Towards clinical application of artificial intelligence in ultrasound imaging,” *Biomedicines*, vol. 9, no. 7, 2021. doi: 10.3390/biomedicines9070720.
- [33] W. M. Dos Santos, S. R. Secoli, and V. A. de A. Püschel, “The Joanna Briggs Institute approach for systematic reviews,” *Rev. Lat. Am. Enfermagem*, vol. 26, p. e3074, 2018. doi: 10.1590/1518-8345.2885.3074.
- [34] A. Liberati et al., “The PRISMA statement for reporting systematic reviews and meta-analyses of studies that evaluate health care interventions: explanation and elaboration,” *J. Clin. Epidemiol.*, vol. 62, no. 10, pp. e1–e34, 2009. doi: 10.1016/j.jclinepi.2009.06.006.
- [35] M. Ouzzani, H. Hammady, Z. Fedorowicz, and A. Elmagarmid, “Rayyan-a web and mobile app for systematic reviews,” *Syst. Rev.*, vol. 5, no. 1, Dec. 2016. doi: 10.1186/s13643-016-0384-4.
- [36] P. Kokol, H. Blažun Vošner, and J. Završnik, “Application of bibliometrics in medicine: a historical bibliometrics analysis,” *Health Info. Libr. J.*, vol. 38, no. 2, pp. 125–138, Jun. 2021. doi: 10.1111/hir.12295.
- [37] M. Bethune, E. Alibrahim, B. Davies, and E. Yong, “A pictorial guide for the second trimester ultrasound,” *Australas. J. Ultrasound Med.*, vol. 16, no. 3, pp. 98–113, Aug. 2013. doi: 10.1002/j.2205-0140.2013.tb00106.x.
- [38] G. Masselli et al., “Imaging for acute pelvic pain in pregnancy,” *Insights Imaging*, vol. 5, no. 2, pp. 165–181, 2014. doi: 10.1007/s13244-014-0314-8.
- [39] D. A. Driscoll and S. Gross, “Prenatal Screening for Aneuploidy,” *N. Engl. J. Med.*, vol. 360, no. 24, pp. 2556–2562, Jun. 2009. doi: 10.1056/nejmcp0900134.
- [40] Q. Huang and Z. Zeng, “A Review on Real-Time 3D Ultrasound Imaging Technology,” *Biomed Res. Int.*, vol. 2017, 2017. doi: 10.1155/2017/6027029.
- [41] J. S. Abramowicz, “Nonmedical use of ultrasound: Bioeffects and safety risk,” *Ultrasound Med. Biol.*, vol. 36, no. 8, pp. 1213–1220, 2010. doi: 10.1016/j.ultrasmedbio.2010.04.003.
- [42] J. Abramowicz, “ALARA: The Clinical View,” *Ultrasound Med. Biol.*, vol. 41, no. 4, p. S102, 2015. doi: 10.1016/j.ultrasmedbio.2014.12.677.
- [43] D. Dowdy, “Keepsake ultrasound: Taking another look,” *J. Radiol. Nurs.*, vol. 35, no. 2, pp. 119–132, Jun. 2016. doi: 10.1016/j.jradnu.2016.02.006.
- [44] A. Kurjak, B. Miskovic, W. Andonotopo, M. Stanojevic, G. Azumendi, and H. Vrcic, “How useful is 3D and 4D ultrasound in perinatal medicine?,” *J. Perinat. Med.*, vol. 35, no. 1, pp. 10–27, Feb. 2007. doi: 10.1515/JPM.2007.002.
- [45] C. Payan, O. Abraham, and V. Garnier, “Ultrasonic Methods,” in *Non-destructive Testing and Evaluation of Civil Engineering Structures*, Elsevier, 2018, pp. 21–85. doi: 10.1016/B978-1-78548-229-8.50002-9.
- [46] L. Mack, “What are the differences between 2D, 3D and 4D ultrasounds scans?,” 2017.

- <https://www.forlongmedical.com/What-are-the-differences-between-2D-3D-and-4D-ultrasounds-scans-id529841.html> (accessed Nov. 06, 2021).
- [47] W. Wang *et al.*, “Medical Image Classification Using Deep Learning,” *Intell. Syst. Ref. Libr.*, vol. 171, pp. 33–51, 2020, doi: 10.1007/978-3-030-32606-7_3.
- [48] S. Asgari Taghanaki, K. Abhishek, J. P. Cohen, J. Cohen-Adad, and G. Hamarneh, “Deep semantic segmentation of natural and medical images: a review,” *Artif. Intell. Rev.*, vol. 54, no. 1, pp. 137–178, Jun. 2021, doi: 10.1007/s10462-020-09854-1.
- [49] A. Bali and S. N. Singh, “A review on the strategies and techniques of image segmentation,” in *International Conference on Advanced Computing and Communication Technologies, ACCT*, Apr. 2015, vol. 2015-April, pp. 113–120. doi: 10.1109/ACCT.2015.63.
- [50] M. H. Hesamian, W. Jia, X. He, and P. Kennedy, “Deep Learning Techniques for Medical Image Segmentation: Achievements and Challenges,” *J. Digit. Imaging*, vol. 32, no. 4, pp. 582–596, Aug. 2019, doi: 10.1007/s10278-019-00227-x.
- [51] F. Sahba, H. R. Tizhoosh, and M. M. A. Salama, “A reinforcement learning framework for medical image segmentation,” in *IEEE International Conference on Neural Networks - Conference Proceedings*, 2006, pp. 511–517. doi: 10.1109/ijcnn.2006.246725.
- [52] S. K. Zhou, H. N. Le, K. Luu, H. V. Nguyen, and N. Ayache, “Deep reinforcement learning in medical imaging: A literature review,” *Med. Image Anal.*, vol. 73, p. 102193, Oct. 2021, doi: 10.1016/j.media.2021.102193.
- [53] M. A. Maraci, R. Napolitano, A. Papageorgiou, and J. A. Noble, “Fisher vector encoding for detecting objects of interest in ultrasound videos,” in *Proceedings - International Symposium on Biomedical Imaging*, 2015, vol. 2015-July, pp. 651–654. doi: 10.1109/ISBI.2015.7163957.
- [54] Y. Gao and J. A. Noble, “Learning and Understanding Deep Spatio-Temporal Representations from Free-Hand Fetal Ultrasound Sweeps,” in *Lecture Notes in Computer Science (including subseries Lecture Notes in Artificial Intelligence and Lecture Notes in Bioinformatics)*, vol. 11768 LNCS, 2019, pp. 299–308. doi: 10.1007/978-3-030-32254-0_34.
- [55] M. Yaqub, B. Kelly, A. T. Papageorgiou, and J. A. Noble, “Guided Random Forests for identification of key fetal anatomy and image categorization in ultrasound scans,” in *Lecture Notes in Computer Science (including subseries Lecture Notes in Artificial Intelligence and Lecture Notes in Bioinformatics)*, 2015, vol. 9351, pp. 687–694. doi: 10.1007/978-3-319-24574-4_82.
- [56] Y. Cai, H. Sharma, P. Chatelain, and J. A. Noble, “Multi-task SonoEyeNet: Detection of fetal standardized planes assisted by generated sonographer attention maps,” *Lect. Notes Comput. Sci. (including Subser. Lect. Notes Artif. Intell. Lect. Notes Bioinformatics)*, vol. 11070 LNCS, pp. 871–879, Sep. 2018, doi: 10.1007/978-3-030-00928-1_98.
- [57] Y. Cai *et al.*, “Spatio-temporal visual attention modelling of standard biometry plane-finding navigation,” *Med. Image Anal.*, vol. 65, p. 101762, Oct. 2020, doi: 10.1016/j.media.2020.101762.
- [58] P. Sridar, A. Kumar, A. Quinton, R. Nanan, J. Kim, and R. Krishnakumar, “Decision Fusion-Based Fetal Ultrasound Image Plane Classification Using Convolutional Neural Networks,” *Ultrasound Med. Biol.*, vol. 45, no. 5, pp. 1259–1273, 2019, doi: 10.1016/j.ultrasmedbio.2018.11.016.
- [59] H. Chen *et al.*, “Ultrasound Standard Plane Detection Using a Composite Neural Network Framework,” *IEEE Trans. Cybern.*, vol. 47, no. 6, pp. 1576–1583, 2017, doi: 10.1109/TCYB.2017.2685080.
- [60] H. Chen *et al.*, “Automatic fetal ultrasound standard plane detection using knowledge transferred recurrent neural networks,” in *Lecture Notes in Computer Science (including subseries Lecture Notes in Artificial Intelligence and Lecture Notes in Bioinformatics)*, 2015, vol. 9349, pp. 507–514. doi: 10.1007/978-3-319-24553-9_62.
- [61] X. P. Burgos-Artizazu *et al.*, “Evaluation of deep convolutional neural networks for automatic classification of common maternal fetal ultrasound planes,” *Sci. Rep.*, vol. 10, no. 1, pp. 1–12, 2020, doi: 10.1038/s41598-020-67076-5.
- [62] R. Liu *et al.*, “NHBS-Net: A Feature Fusion Attention Network for Ultrasound Neonatal Hip Bone Segmentation,” *IEEE Trans. Med. Imaging*, 2021, doi: 10.1109/TMI.2021.3087857.
- [63] N. H. Weerasinghe, N. H. Lovell, A. W. Welsh, and G. N. Stevenson, “Multi-Parametric Fusion of 3D Power Doppler Ultrasound for Fetal Kidney Segmentation Using Fully Convolutional Neural Networks,” *IEEE J. Biomed. Heal. Informatics*, vol. 25, no. 6, pp. 2050–2057, 2021, doi: 10.1109/JBHI.2020.3027318.
- [64] R. Rahmatullah, M. A. Ma’Sum, Aprinaldi, P. Mursanto, and B. Wiweko, “Automatic fetal organs segmentation using multilayer super pixel and image moment feature,” in *Proceedings - ICACISIS 2014: 2014 International Conference on Advanced Computer Science and Information Systems*, 2014, pp. 420–426. doi: 10.1109/ICACISIS.2014.7065883.
- [65] H. Ryou, M. Yaqub, A. Cavallaro, A. T. Papageorgiou, and J. Alison Noble, “Automated 3D ultrasound image analysis for first trimester assessment of fetal health,” *Phys. Med. Biol.*, vol. 64, no. 18, p. 185010, 2019, doi: 10.1088/1361-6560/ab3ad1.
- [66] H. Ryou, M. Yaqub, A. Cavallaro, F. Roseman, A. Papageorgiou, and J. Alison Noble, “Automated 3D ultrasound biometry planes extraction for first trimester fetal assessment,” in *Lecture Notes in Computer Science (including subseries Lecture Notes in Artificial Intelligence and Lecture Notes in Bioinformatics)*, Oct. 2016, vol. 10019 LNCS, pp. 196–204. doi: 10.1007/978-3-319-47157-0_24.
- [67] N. Toussaint *et al.*, “Weakly supervised localisation for fetal ultrasound images,” in *Lecture Notes in Computer Science (including subseries Lecture Notes in Artificial Intelligence and Lecture Notes in Bioinformatics)*, vol. 11045 LNCS, Springer, 2018, pp. 192–200. doi: 10.1007/978-3-030-00889-5_22.
- [68] H. Ravishanker, S. M. Prabhu, V. Vaidya, and N. Singhal, “Hybrid approach for automatic segmentation of fetal abdomen from ultrasound images using deep learning,” in *Proceedings - International Symposium on Biomedical Imaging*, 2016, vol. 2016-June, pp. 779–782. doi: 10.1109/ISBI.2016.7493382.
- [69] L. K. Wee, T. Y. Min, A. Arooj, and E. Supriyanto, “Nuchal translucency marker detection based on artificial neural network and measurement via bidirectional iteration forward propagation,” *WSEAS Trans. Inf. Sci. Appl.*, vol. 7, no. 8, pp. 1025–1036, 2010.
- [70] X. Yang *et al.*, “Towards automated semantic segmentation in prenatal volumetric ultrasound,” *IEEE Trans. Med. Imaging*, vol. 38, no. 1, pp. 180–193, 2019, doi: 10.1109/TMI.2018.2858779.
- [71] P. Looney *et al.*, “Fully Automated 3-D Ultrasound Segmentation of the Placenta, Amniotic Fluid, and Fetus for Early Pregnancy Assessment,” *IEEE Trans. Ultrason. Ferroelectr. Freq. Control*, vol. 68, no. 6, pp. 2038–2047, 2021, doi: 10.1109/TUFFC.2021.3052143.
- [72] Y. Li, R. Xu, J. Ohya, and H. Iwata, “Automatic fetal body and amniotic fluid segmentation from fetal ultrasound images by encoder-decoder network with inner layers,” in *Proceedings of the Annual International Conference of the IEEE Engineering in Medicine and Biology Society, EMBS*, 2017, pp. 1485–1488. doi: 10.1109/EMBC.2017.8037116.
- [73] T. Liu *et al.*, “Direct detection and measurement of nuchal translucency with neural networks from ultrasound images,” in *Lecture Notes in Computer Science (including subseries Lecture Notes in Artificial Intelligence and Lecture Notes in Bioinformatics)*, vol. 11798 LNCS, Springer, 2019, pp. 20–28. doi: 10.1007/978-3-030-32875-7_3.
- [74] K. S. Bagi and K. S. Shreedhara, “Biometric measurement and classification of IUGR using neural networks,” in *Proceedings of 2014 International Conference on Contemporary Computing and Informatics, IC3I 2014*, 2014, pp. 157–161. doi: 10.1109/IC3I.2014.7019613.
- [75] D. Selvathi and R. Chandralekha, “Fetal biometric based abnormality detection during prenatal development using deep learning techniques,” *Multidimens. Syst. Signal Process.*, 2021, doi: 10.1007/s11045-021-00765-0.
- [76] F. Andriani and I. Mardiyah, “Blighted Ovum detection using convolutional neural network,” in *AIP Conference Proceedings*, vol. 2084, 2019. doi: 10.1063/1.5094276.
- [77] R. Yekdast, “An Intelligent Method for Down Syndrome Detection in Fetuses Using Ultrasound Images and Deep Learning Neural Networks,” *Comput. Res. Prog. Appl. Sci. Eng.*, vol. 5, no. 3, pp. 92–97, 2019.
- [78] V. Rawat, A. Jain, V. Shrimali, and A. Rawat, “Automatic detection of fetal abnormality using head and abdominal circumference,” in *Lecture Notes in Computer Science (including subseries Lecture Notes in Artificial Intelligence and Lecture Notes in Bioinformatics)*, vol. 9876 LNCS, N. T. Nguyen, Y. Manolopoulos, L. Iliadis, and B. Trawinski, Eds. 2016, pp. 525–534. doi: 10.1007/978-3-319-45246-3_50.
- [79] A. V. Gadagkar and K. S. Shreedhara, “Features based IUGR

- diagnosis using variational level set method and classification using artificial neural networks,” in *Proceedings - 2014 5th International Conference on Signal and Image Processing, ICSIP 2014*, 2014, pp. 303–309. doi: 10.1109/ICSIP.2014.54.
- [80] M. A. Maraci et al., “Toward point-of-care ultrasound estimation of fetal gestational age from the trans-cerebellar diameter using CNN-based ultrasound image analysis,” *J. Med. Imaging*, vol. 7, no. 01, p. 1, 2020, doi: 10.1117/1.jmi.7.1.014501.
- [81] P. Chen et al., “A preliminary study to quantitatively evaluate the development of maturation degree for fetal lung based on transfer learning deep model from ultrasound images,” *Int. J. Comput. Assist. Radiol. Surg.*, vol. 15, no. 8, pp. 1407–1415, Aug. 2020, doi: 10.1007/s11548-020-02211-1.
- [82] J. C. Prieto et al., “An automated framework for image classification and segmentation of fetal ultrasound images for gestational age estimation,” *Proc. SPIE--the Int. Soc. Opt. Eng.*, vol. 11596, p. 55, Feb. 2021, doi: 10.1117/12.2582243.
- [83] I. M. D. Maysanjaya, H. A. Nugroho, and N. A. Setiawan, “The classification of fetus gender on ultrasound images using learning vector quantization (LVQ),” in *Proceeding - 2014 Makassar International Conference on Electrical Engineering and Informatics, MICEEI 2014*, 2014, pp. 150–155. doi: 10.1109/MICEEI.2014.7067329.
- [84] S. Nie, J. Yu, P. Chen, J. Zhang, and Y. Wang, “A novel method with a deep network and directional edges for automatic detection of a fetal head,” in *2015 23rd European Signal Processing Conference, EUSIPCO 2015*, 2015, pp. 654–658. doi: 10.1109/EUSIPCO.2015.7362464.
- [85] J. Li et al., “Automatic Fetal Head Circumference Measurement in Ultrasound Using Random Forest and Fast Ellipse Fitting,” *IEEE J. Biomed. Heal. Informatics*, vol. 22, no. 1, pp. 215–223, 2018, doi: 10.1109/JBHI.2017.2703890.
- [86] S. Nie, J. Yu, Y. Wang, J. Zhang, and P. Chen, “Shape model and marginal space of 3D ultrasound volume data for automatically detecting a fetal head,” in *ICALIP 2014 - 2014 International Conference on Audio, Language and Image Processing, Proceedings*, 2015, pp. 681–685. doi: 10.1109/ICALIP.2014.7009881.
- [87] Z. Sobhaninia, A. Emami, N. Karimi, and S. Samavi, “Localization of Fetal Head in Ultrasound Images by Multiscale View and Deep Neural Networks,” in *2020 25th International Computer Conference, Computer Society of Iran, CSICC 2020*, 2020, pp. 1–5. doi: 10.1109/CSICC49403.2020.9050094.
- [88] C. P. Aji, M. H. Fatoni, and T. A. Sardjono, “Automatic Measurement of Fetal Head Circumference from 2-Dimensional Ultrasound,” in *2019 International Conference on Computer Engineering, Network, and Intelligent Multimedia, CENIM 2019 - Proceeding*, 2019, vol. 2019-Novem, pp. 1–5. doi: 10.1109/CENIM48368.2019.8973258.
- [89] Y. Zeng, P. H. Tsui, W. Wu, Z. Zhou, and S. Wu, “Fetal Ultrasound Image Segmentation for Automatic Head Circumference Biometry Using Deeply Supervised Attention-Gated V-Net,” *J. Digit. Imaging*, vol. 34, no. 1, pp. 134–148, Feb. 2021, doi: 10.1007/s10278-020-00410-5.
- [90] J. Perez-Gonzalez, N. Hevia Montiel, and V. M. Bañuelos, “Deep Learning Spatial Compounding from Multiple Fetal Head Ultrasound Acquisitions,” in *Lecture Notes in Computer Science (including subseries Lecture Notes in Artificial Intelligence and Lecture Notes in Bioinformatics)*, vol. 12437 LNCS, Springer, 2020, pp. 305–314. doi: 10.1007/978-3-030-60334-2_30.
- [91] L. Xu et al., “Exploiting vector attention and context prior for ultrasound image segmentation,” *Neurocomputing*, vol. 454, pp. 461–473, 2021, doi: 10.1016/j.neucom.2021.05.033.
- [92] E. L. Skeika, M. R. da Luz, B. J. Torres Fernandes, H. V. Siqueira, and M. L. S. C. de Andrade, “Convolutional neural network to detect and measure fetal skull circumference in ultrasound imaging,” *IEEE Access*, vol. 8, pp. 191519–191529, 2020, doi: 10.1109/ACCESS.2020.3032376.
- [93] A. I. L. Namburete and J. A. Noble, “Fetal cranial segmentation in 2D ultrasound images using shape properties of pixel clusters,” in *Proceedings - International Symposium on Biomedical Imaging*, 2013, pp. 720–723. doi: 10.1109/ISBI.2013.6556576.
- [94] S. Budd et al., “Confident head circumference measurement from ultrasound with real-time feedback for sonographers,” in *Lecture Notes in Computer Science (including subseries Lecture Notes in Artificial Intelligence and Lecture Notes in Bioinformatics)*, 2019, vol. 11767 LNCS, pp. 683–691. doi: 10.1007/978-3-030-32251-9_75.
- [95] A. Desai, R. Chauhan, and J. Sivaswamy, “Image Segmentation Using Hybrid Representations,” in *Proceedings - International Symposium on Biomedical Imaging*, 2020, vol. 2020-April, pp. 1513–1516. doi: 10.1109/ISBI45749.2020.9098463.
- [96] K. Brahma, V. Kumar, A. E. Samir, A. P. Chandrakasan, and Y. C. Eldar, “Efficient binary cnn for medical image segmentation,” in *Proceedings - International Symposium on Biomedical Imaging*, 2021, vol. 2021-April, pp. 817–821. doi: 10.1109/ISBI48211.2021.9433901.
- [97] D. Qiao and F. Zulkernine, “Dilated Squeeze-and-Excitation U-Net for Fetal Ultrasound Image Segmentation,” in *2020 IEEE Conference on Computational Intelligence in Bioinformatics and Computational Biology, CIBCB 2020*, 2020, pp. 1–7. doi: 10.1109/CIBCB48159.2020.9277667.
- [98] Z. Sobhaninia et al., “Fetal Ultrasound Image Segmentation for Measuring Biometric Parameters Using Multi-Task Deep Learning,” in *Proceedings of the Annual International Conference of the IEEE Engineering in Medicine and Biology Society, EMBS, 2019*, pp. 6545–6548. doi: 10.1109/EMBC.2019.8856981.
- [99] L. Zhang, J. Zhang, Z. Li, and Y. Song, “A multiple-channel and atrous convolution network for ultrasound image segmentation,” *Med. Phys.*, vol. 47, no. 12, pp. 6270–6285, Dec. 2020, doi: 10.1002/mp.14512.
- [100] M. Sinclair et al., “Human-level Performance on Automatic Head Biometrics in Fetal Ultrasound Using Fully Convolutional Neural Networks,” in *Proceedings of the Annual International Conference of the IEEE Engineering in Medicine and Biology Society, EMBS, 2018*, vol. 2018-July, pp. 714–717. doi: 10.1109/EMBC.2018.8512278.
- [101] J. J. Cerrolaza et al., “Deep learning with ultrasound physics for fetal skull segmentation,” in *Proceedings - International Symposium on Biomedical Imaging*, 2018, vol. 2018-April, pp. 564–567. doi: 10.1109/ISBI.2018.8363639.
- [102] P. Li, H. Zhao, P. Liu, and F. Cao, “Automated measurement network for accurate segmentation and parameter modification in fetal head ultrasound images,” *Med. Biol. Eng. Comput.*, vol. 58, no. 11, pp. 2879–2892, Nov. 2020, doi: 10.1007/s11517-020-02242-5.
- [103] R. Droste, P. Chatelain, L. Drukker, H. Sharma, A. T. Papageorghiou, and J. A. Noble, “Discovering Salient Anatomical Landmarks by Predicting Human Gaze,” in *Proceedings - International Symposium on Biomedical Imaging*, 2020, vol. 2020-April, pp. 1711–1714. doi: 10.1109/ISBI45749.2020.9098505.
- [104] B. Al-Bander, T. Alzahrani, S. Alzahrani, B. M. Williams, and Y. Zheng, “Improving Fetal Head Contour Detection by Object Localisation with Deep Learning,” in *Communications in Computer and Information Science*, 2020, vol. 1065 CCIS, pp. 142–150. doi: 10.1007/978-3-030-39343-4_12.
- [105] M. C. Fiorentino, S. Moccia, M. Capparuccini, S. Giamberini, and E. Frontoni, “A regression framework to head-circumference delineation from US fetal images,” *Comput. Methods Programs Biomed.*, vol. 198, p. 105771, Jan. 2021, doi: 10.1016/j.cmpb.2020.105771.
- [106] S. Fathimuthu Joharah and K. Mohideen, “Automatic detection of fetal ultrasound image using multi-task deep learning,” *J. Crit. Rev.*, vol. 7, no. 7, pp. 987–993, 2020, doi: 10.31838/jcr.07.07.181.
- [107] R. Qu, G. Xu, C. Ding, W. Jia, and M. Sun, “Deep Learning-Based Methodology for Recognition of Fetal Brain Standard Scan Planes in 2D Ultrasound Images,” *IEEE Access*, vol. 8, pp. 44443–44451, 2020, doi: 10.1109/ACCESS.2019.2950387.
- [108] R. Qu, G. Xu, C. Ding, W. Jia, and M. Sun, “Standard plane identification in fetal brain ultrasound scans using a differential convolutional neural network,” *IEEE Access*, vol. 8, pp. 83821–83830, 2020, doi: 10.1109/ACCESS.2020.2991845.
- [109] V. Singh et al., “Semantic Segmentation of Cerebellum in 2D Fetal Ultrasound Brain Images Using Convolutional Neural Networks,” *IEEE Access*, vol. 9, pp. 85864–85873, 2021, doi: 10.1109/access.2021.3088946.
- [110] S. Wang et al., “Deep Learning based Fetal Middle Cerebral Artery Segmentation in Large-scale Ultrasound Images,” in *Proceedings - 2018 IEEE International Conference on Bioinformatics and Biomedicine, BIBM 2018*, 2019, pp. 532–539. doi: 10.1109/BIBM.2018.8621510.
- [111] M. Yaqub et al., “Volumetric segmentation of key fetal brain structures in 3D ultrasound,” in *Lecture Notes in Computer Science (including subseries Lecture Notes in Artificial Intelligence and Lecture Notes in Bioinformatics)*, vol. 8184

- LNCs, 2013, pp. 25–32. doi: 10.1007/978-3-319-02267-3_4.
- [112] A. I. L. Namburete, W. Xie, M. Yaqub, A. Zisserman, and J. A. Noble, “Fully-automated alignment of 3D fetal brain ultrasound to a canonical reference space using multi-task learning,” *Med. Image Anal.*, vol. 46, pp. 1–14, 2018, doi: 10.1016/j.media.2018.02.006.
- [113] R. Huang, W. Xie, and J. Alison Noble, “VP-Nets: Efficient automatic localization of key brain structures in 3D fetal neurosonography,” *Med. Image Anal.*, vol. 47, pp. 127–139, 2018, doi: 10.1016/j.media.2018.04.004.
- [114] R. Cuingnet *et al.*, “Where is my baby? A fast fetal head auto-alignment in 3D-ultrasound,” in *Proceedings - International Symposium on Biomedical Imaging*, 2013, pp. 768–771. doi: 10.1109/ISBI.2013.6556588.
- [115] X. Yang *et al.*, “Agent with Warm Start and Adaptive Dynamic Termination for Plane Localization in 3D Ultrasound,” *IEEE Trans. Med. Imaging*, vol. 11768, pp. 290–298, 2021, doi: 10.1109/TMI.2021.3069663.
- [116] X. Yang *et al.*, “Searching collaborative agents for multi-plane localization in 3D ultrasound,” *Med. Image Anal.*, vol. 72, p. 102119, May 2021, doi: 10.1016/j.media.2021.102119.
- [117] Z. Lin *et al.*, “Quality assessment of fetal head ultrasound images based on faster R-CNN,” *Chinese J. Biomed. Eng.*, vol. 38, no. 4, pp. 392–400, 2019, doi: 10.3969/j.issn.0258-8021.2019.04.002.
- [118] Z. Lin *et al.*, “Multi-task learning for quality assessment of fetal head ultrasound images,” *Med. Image Anal.*, vol. 58, p. 101548, Dec. 2019, doi: 10.1016/j.media.2019.101548.
- [119] H. P. Kim, S. M. Lee, J. Y. Kwon, Y. Park, K. C. Kim, and J. K. Seo, “Automatic evaluation of fetal head biometry from ultrasound images using machine learning,” *Physiol. Meas.*, vol. 40, no. 6, p. 65009, 2019, doi: 10.1088/1361-6579/ab21ac.
- [120] H. Sahli, M. Sayadi, and R. Rachdi, “Intelligent detection of fetal hydrocephalus,” *Comput. Methods Biomech. Biomed. Eng. Imaging Vis.*, vol. 8, no. 6, pp. 641–648, 2020, doi: 10.1080/21681163.2020.1780156.
- [121] H. N. Xie *et al.*, “Using deep-learning algorithms to classify fetal brain ultrasound images as normal or abnormal,” *Ultrasound Obstet. Gynecol.*, vol. 56, no. 4, pp. 579–587, 2020, doi: 10.1002/uog.21967.
- [122] B. Xie *et al.*, “Computer-aided diagnosis for fetal brain ultrasound images using deep convolutional neural networks,” *Int. J. Comput. Assist. Radiol. Surg.*, vol. 15, no. 8, pp. 1303–1312, Aug. 2020, doi: 10.1007/s11548-020-02182-3.
- [123] R. Liu *et al.*, “Automated fetal lateral ventricular width estimation from prenatal ultrasound based on deep learning algorithms,” *Authorea Prepr.*, May 2020, doi: 10.22541/AU.158872369.94920854.
- [124] X. Chen *et al.*, “Automatic Measurements of Fetal Lateral Ventricles in 2D Ultrasound Images Using Deep Learning,” *Front. Neurol.*, vol. 11, p. 526, 2020, doi: 10.3389/fneur.2020.00526.
- [125] B. Lei, L. Zhuo, S. Chen, S. Li, D. Ni, and T. Wang, “Automatic recognition of fetal standard plane in ultrasound image,” in *2014 IEEE 11th International Symposium on Biomedical Imaging, ISBI 2014*, 2014, pp. 85–88. doi: 10.1109/isbi.2014.6867815.
- [126] Z. Yu, D. Ni, S. Chen, S. Li, T. Wang, and B. Lei, “Fetal facial standard plane recognition via very deep convolutional neural networks,” in *Proceedings of the Annual International Conference of the IEEE Engineering in Medicine and Biology Society, EMBS*, 2016, vol. 2016-October, pp. 627–630. doi: 10.1109/EMBC.2016.7590780.
- [127] Z. Yu *et al.*, “A deep convolutional neural network-based framework for automatic fetal facial standard plane recognition,” *IEEE J. Biomed. Heal. Informatics*, vol. 22, no. 3, pp. 874–885, 2018, doi: 10.1109/JBHI.2017.2705031.
- [128] B. Lei *et al.*, “Automatic recognition of fetal facial standard plane in ultrasound image via Fisher vector,” *PLoS One*, vol. 10, no. 5, p. e0121838, 2015, doi: 10.1371/journal.pone.0121838.
- [129] X. Wang *et al.*, “Recognition of Fetal Facial Ultrasound Standard Plane Based on Texture Feature Fusion,” *Comput. Math. Methods Med.*, vol. 2021, 2021, doi: 10.1155/2021/6656942.
- [130] T. Singh, S. R. Kudavelly, and K. V. Suryanarayana, “Deep learning based fetal face detection and visualization in prenatal ultrasound,” in *Proceedings - International Symposium on Biomedical Imaging*, 2021, vol. 2021-April, pp. 1760–1763. doi: 10.1109/ISBI48211.2021.9433915.
- [131] C. Chen *et al.*, “Region Proposal Network with Graph Prior and Iou-Balance Loss for Landmark Detection in 3D Ultrasound,” in *Proceedings - International Symposium on Biomedical Imaging*, 2020, vol. 2020-April, pp. 1829–1833. doi: 10.1109/ISBI45749.2020.9098368.
- [132] T. A. Anjit and S. Rishidas, “Identification of nasal bone for the early detection of down syndrome using Back Propagation Neural Network,” in *ICCSP 2011 - 2011 International Conference on Communications and Signal Processing*, 2011, pp. 136–140. doi: 10.1109/ICCSP.2011.5739286.
- [133] P. R. Dave and M. S. B. Nadiad, “Facial expressions extraction from 3D sonography images,” in *Proceedings of 2015 IEEE International Conference on Electrical, Computer and Communication Technologies, ICECCT 2015*, 2015, pp. 1–6. doi: 10.1109/ICECCT.2015.7226070.
- [134] Y. Miyagi, T. Hata, S. Bouno, A. Koyanagi, and T. Miyake, “Recognition of facial expression of fetuses by artificial intelligence (AI),” *J. Perinat. Med.*, vol. 49, no. 5, pp. 596–603, Jun. 2021, doi: 10.1515/jpm-2020-0537.
- [135] M. Dinesh Simon and A. R. Kavitha, “Ultrasonic Detection of Down Syndrome Using Multiscale Quantiser with Convolutional Neural Network,” in *Computational Optimization Techniques and Applications*, IntechOpen, 2021. doi: 10.5772/intechopen.96502.
- [136] J. Tan *et al.*, “Automated Detection of Congenital Heart Disease in Fetal Ultrasound Screening,” in *Lecture Notes in Computer Science (including subseries Lecture Notes in Artificial Intelligence and Lecture Notes in Bioinformatics)*, vol. 12437 LNCS, Springer, 2020, pp. 243–252. doi: 10.1007/978-3-030-60334-2_24.
- [137] T. Yang *et al.*, “Segmentation of Five Components in Four Chamber View of Fetal Echocardiography,” in *Proceedings - International Symposium on Biomedical Imaging*, 2020, vol. 2020-April, pp. 1962–1965. doi: 10.1109/ISBI45749.2020.9098726.
- [138] R. Arnaout, L. Curran, Y. Zhao, J. C. Levine, E. Chinn, and A. J. Moon-Grady, “An ensemble of neural networks provides expert-level prenatal detection of complex congenital heart disease,” *Nat. Med.*, vol. 27, no. 5, pp. 882–891, 2021, doi: 10.1038/s41591-021-01342-5.
- [139] Y. Gong *et al.*, “Fetal congenital heart disease echocardiogram screening based on dgacnn: Adversarial one-class classification combined with video transfer learning,” *IEEE Trans. Med. Imaging*, vol. 39, no. 4, pp. 1206–1222, 2020, doi: 10.1109/TMI.2019.2946059.
- [140] M. Komatsu *et al.*, “Detection of cardiac structural abnormalities in fetal ultrasound videos using deep learning,” *Appl. Sci.*, vol. 11, no. 1, pp. 1–12, 2021, doi: 10.3390/app11010371.
- [141] A. Dozen *et al.*, “Image segmentation of the ventricular septum in fetal cardiac ultrasound videos based on deep learning using time-series information,” *Biomolecules*, vol. 10, no. 11, pp. 1–17, 2020, doi: 10.3390/biom10111526.
- [142] A. Patra, W. Huang, and J. A. Noble, “Learning spatio-temporal aggregation for fetal heart analysis in ultrasound video,” in *Lecture Notes in Computer Science (including subseries Lecture Notes in Artificial Intelligence and Lecture Notes in Bioinformatics)*, vol. 10553 LNCS, Springer, 2017, pp. 276–284. doi: 10.1007/978-3-319-67558-9_32.
- [143] L. Xu, M. Liu, J. Zhang, and Y. He, “Convolutional-Neural-Network-Based Approach for Segmentation of Apical Four-Chamber View from Fetal Echocardiography,” *IEEE Access*, vol. 8, pp. 80437–80446, 2020, doi: 10.1109/ACCESS.2020.2984630.
- [144] L. Xu *et al.*, “DW-Net: A cascaded convolutional neural network for apical four-chamber view segmentation in fetal echocardiography,” *Comput. Med. Imaging Graph.*, vol. 80, p. 101690, Mar. 2020, doi: 10.1016/j.compmedimag.2019.101690.
- [145] V. Sundaresan, C. P. Bridge, C. Ioannou, and J. A. Noble, “Automated characterization of the fetal heart in ultrasound images using fully convolutional neural networks,” in *Proceedings - International Symposium on Biomedical Imaging*, 2017, pp. 671–674. doi: 10.1109/ISBI.2017.7950609.
- [146] J. Dong *et al.*, “A Generic Quality Control Framework for Fetal Ultrasound Cardiac Four-Chamber Planes,” *IEEE J. Biomed. Heal. Informatics*, vol. 24, no. 4, pp. 931–942, 2020, doi: 10.1109/JBHI.2019.2948316.
- [147] B. Pu, N. Zhu, K. Li, and S. Li, “Fetal cardiac cycle detection in multi-resource echocardiograms using hybrid classification framework,” *Futur. Gener. Comput. Syst.*, vol. 115, pp. 825–836, 2021, doi: 10.1016/j.future.2020.09.014.
- [148] B. Rahmatullah, I. Sarris, A. Papageorghiou, and J. A. Noble, “Quality control of fetal ultrasound images: Detection of abdomen anatomical landmarks using AdaBoost,” in *Proceedings -*

- International Symposium on Biomedical Imaging*, 2011, pp. 6–9. doi: 10.1109/ISBI.2011.5872342.
- [149] X. Yang et al., “Standard plane localization in ultrasound by radial component,” in *2014 IEEE 11th International Symposium on Biomedical Imaging, ISBI 2014*, 2014, pp. 1180–1183. doi: 10.1109/isbi.2014.6868086.
- [150] L. Wu, J. Z. Cheng, S. Li, B. Lei, T. Wang, and D. Ni, “FUIQA: Fetal ultrasound image quality assessment with deep convolutional networks,” *IEEE Trans. Cybern.*, vol. 47, no. 5, pp. 1336–1349, 2017, doi: 10.1109/TCYB.2017.2671898.
- [151] D. Ni et al., “Standard Plane Localization in Ultrasound by Radial Component Model and Selective Search,” *Ultrasound Med. Biol.*, vol. 40, no. 11, pp. 2728–2742, Nov. 2014, doi: 10.1016/j.ultrasmedbio.2014.06.006.
- [152] B. Rahmatnillah, A. T. Papageorghiou, and J. Alison Noble, “Image analysis using machine learning: Anatomical landmarks detection in fetal ultrasound images,” in *Proceedings - International Computer Software and Applications Conference*, 2012, pp. 354–355. doi: 10.1109/COMPSAC.2012.52.
- [153] H. Chen, D. Ni, X. Yang, S. Li, and P. A. Heng, “Fetal Abdominal Standard Plane Localization Through Representation Learning with Knowledge Transfer,” in *Lecture Notes in Computer Science (including subseries Lecture Notes in Artificial Intelligence and Lecture Notes in Bioinformatics)*, vol. 8679, 2014, pp. 125–132. doi: 10.1007/978-3-319-10581-9_16.
- [154] B. Rahmatullah, A. Papageorghiou, and J. A. Noble, “Automated selection of standardized planes from ultrasound volume,” in *Lecture Notes in Computer Science (including subseries Lecture Notes in Artificial Intelligence and Lecture Notes in Bioinformatics)*, vol. 7009 LNCS, 2011, pp. 35–42. doi: 10.1007/978-3-642-24319-6_5.
- [155] B. Kim, K. C. Kim, Y. Park, J. Y. Kwon, J. Jang, and J. K. Seo, “Machine-learning-based automatic identification of fetal abdominal circumference from ultrasound images,” *Physiol. Meas.*, vol. 39, no. 10, p. 105007, 2018, doi: 10.1088/1361-6579/aae255.
- [156] P. Deepika, R. M. Suresh, and P. Pabitha, “Defending Against Child Death: Deep learning-based diagnosis method for abnormal identification of fetus ultrasound Images,” *Comput. Intell.*, vol. 37, no. 1, pp. 128–154, 2021, doi: 10.1111/coin.12394.
- [157] J. Jang, Y. Park, B. Kim, S. M. Lee, J. Y. Kwon, and J. K. Seo, “Automatic Estimation of Fetal Abdominal Circumference from Ultrasound Images,” *IEEE J. Biomed. Heal. Informatics*, vol. 22, no. 5, pp. 1512–1520, Nov. 2017, doi: 10.1109/JBHI.2017.2776116.
- [158] B. C. Lowekamp, D. T. Chen, L. Ibáñez, and D. Blezek, “The design of simpleITK,” *Front. Neuroinform.*, vol. 7, no. DEC, p. 45, Dec. 2013, doi: 10.3389/fninf.2013.00045.
- [159] P. Yushkevich, J. Piven, H. Cody, and S. Ho, “User-guided level set segmentation of anatomical structures with ITK-SNAP,” *Neuroimage*, vol. 31, no. 3, pp. 1116–1128, 2006, Accessed: Oct. 03, 2021. [Online]. Available: https://www.academia.edu/download/41218070/User-Guided_Level_Set_Segmentation_of_An20160113-9594-xfzom3.pdf20160115-19908-1771q5v.pdf
- [160] T. L. A. van den Heuvel, D. de Bruijn, C. L. de Korte, and B. van Ginneken, “Automated measurement of fetal head circumference using 2D ultrasound images,” *PLoS One*, vol. 13, no. 8, Aug. 2018, doi: 10.1371/journal.pone.0200412.
- [161] J. Zhang, C. Petitjean, P. Lopez, and S. Ainouz, “Direct estimation of fetal head circumference from ultrasound images based on regression CNN,” in *Proceedings of Machine Learning Research*, 2020, vol. 121, pp. 914–922. [Online]. Available: <http://proceedings.mlr.press/v121/zhang20a.html>
- [162] S. Pieper, M. Halle, and R. Kikinis, “3D Slicer,” in *2004 2nd IEEE International Symposium on Biomedical Imaging: Macro to Nano*, 2004, vol. 1, no. 3, pp. 632–635. doi: 10.1007/s00113-019-0654-4.
- [163] X. Yang et al., “Hybrid attention for automatic segmentation of whole fetal head in prenatal ultrasound volumes,” *Comput. Methods Programs Biomed.*, vol. 194, p. 105519, 2020, doi: 10.1016/j.cmpb.2020.105519.
- [164] C. F. Baumgartner et al., “SonoNet: Real-Time Detection and Localisation of Fetal Standard Scan Planes in Freehand Ultrasound,” *IEEE Trans. Med. Imaging*, vol. 36, no. 11, pp. 2204–2215, Nov. 2017, doi: 10.1109/TMI.2017.2712367.
- [165] N. K. Chauhan and K. Singh, “A review on conventional machine learning vs deep learning,” in *2018 International Conference on Computing, Power and Communication Technologies, GUCON 2018*, Mar. 2019, pp. 347–352. doi: 10.1109/GUCON.2018.8675097.
- [166] K. Yasaka and O. Abe, “Deep learning and artificial intelligence in radiology: Current applications and future directions,” *PLoS Med.*, vol. 15, no. 11, Nov. 2018, doi: 10.1371/journal.pmed.1002707.
- [167] B. Shuo, Wang, M. Ji-Bin, Liu, M. Ziyin, Zhu, and P. John, Eisenbrey, “Artificial Intelligence in Ultrasound Imaging: Current Research and Applications,” *Adv. ULTRASOUND DIAGNOSIS Ther.*, vol. 3, no. 3, p. 53, Sep. 2019, doi: 10.37015/audt.2019.190811.
- [168] Z. Akkus et al., “A Survey of Deep-Learning Applications in Ultrasound: Artificial Intelligence–Powered Ultrasound for Improving Clinical Workflow,” *J. Am. Coll. Radiol.*, vol. 16, no. 9, pp. 1318–1328, 2019, doi: 10.1016/j.jacr.2019.06.004.
- [169] E. Neri et al., “What the radiologist should know about artificial intelligence – an ESR white paper,” *Insights Imaging*, vol. 10, no. 1, Dec. 2019, doi: 10.1186/s13244-019-0738-2.
- [170] D. A. Bluemke et al., “Assessing radiology research on artificial intelligence: A brief guide for authors, reviewers, and readers-from the Radiology Editorial Board,” *Radiology*, vol. 294, no. 2, pp. 487–489, 2020, doi: 10.1148/radiol.2019192515.
- [171] A. Hasan Sapci and H. Aylin Sapci, “Artificial intelligence education and tools for medical and health informatics students: Systematic review,” *JMIR Med. Educ.*, vol. 6, no. 1, 2020, doi: 10.2196/19285.
- [172] I. M. Pires, G. Marques, N. M. Garcia, F. Flórez-revuelta, V. Ponciano, and S. Oniani, “A research on the classification and applicability of the mobile health applications,” *J. Pers. Med.*, vol. 10, no. 1, 2020, doi: 10.3390/jpm10010011.
- [173] D. P. Bahner, A. Jasne, S. Boore, A. Mueller, and E. Cortez, “The ultrasound challenge: a novel approach to medical student ultrasound education,” *J. Ultrasound Med.*, vol. 31, no. 12, pp. 2013–2016, Dec. 2012, doi: 10.7863/jum.2012.31.12.2013.
- [174] J. J. Bartko, “The intraclass correlation coefficient as a measure of reliability,” *Psychol. Rep.*, vol. 19, no. 1, pp. 3–11, Sep. 1966, doi: 10.2466/pr0.1966.19.1.3.